

Reason-RFT: Reinforcement Fine-Tuning for Visual Reasoning of Vision Language Models

Huajie Tan^{1,2,*}, Yuheng Ji^{2,3,4,*}, Xiaoshuai Hao^{2,*}, Xiansheng Chen^{2,*},
Pengwei Wang^{2,†}, Zhongyuan Wang², Shanghang Zhang^{1,2,✉}

¹ State Key Laboratory of Multimedia Information Processing, School of Computer Science, Peking University

² Beijing Academy of Artificial Intelligence ³ Institute of Automation, Chinese Academy of Sciences

⁴ School of Artificial Intelligence, University of Chinese Academy of Sciences

Abstract

Visual reasoning abilities play a crucial role in understanding complex multimodal data, advancing both domain-specific applications and artificial general intelligence (AGI). Existing methods improve Vision-Language Models (VLMs) reasoning via Chain-of-Thought (CoT) supervised fine-tuning, using meticulously annotated training data to enhance visual reasoning capabilities. However, this training paradigm may lead to overfitting and cognitive rigidity, restricting the model’s generalization ability to transfer visual reasoning skills under domain shift and limiting its real-world applicability. To address these limitations, we propose **Reason-RFT**, the first two-stage reinforcement fine-tuning framework for visual reasoning: (1) Supervised Fine-Tuning (SFT) with curated CoT data activates the reasoning potential of VLMs, followed by (2) Group Relative Policy Optimization (GRPO)-based reinforcement learning that generates multiple reasoning-response pairs, significantly enhancing the capability to address ubiquitous domain shift in visual reasoning tasks. To evaluate the visual reasoning capabilities of *Reason-RFT*, we reconstructed a comprehensive dataset encompassing visual counting, structural perception, and spatial transformation, serving as a benchmark for systematic assessment across three core dimensions. Experimental results demonstrate three key advantages: (1) *Performance Enhancement*: achieving state-of-the-art results across multiple tasks, outperforming mainstream open-source and proprietary models; (2) *Generalization Superiority*: consistently maintaining robust performance in addressing domain shift in typical visual reasoning tasks, outperforming alternative paradigms; (3) *Data Efficiency*: excelling in few-shot learning scenarios while surpassing full-dataset SFT baselines. *Reason-RFT* introduces a robust training paradigm in visual reasoning, and please refer to project website: Reason-RFT.

1 Introduction

Visual reasoning is pivotal for understanding complex multimodal data and advancing artificial general intelligence (AGI) [1, 2], making it a central focus in intelligent systems research. Recent advancements in image recognition [3–9], interactive security [10–12] and scene understanding [13, 14] have enabled transformative applications in healthcare [15, 16], robotics [17–24], and autonomous driving [25–31]. Consequently, enhancing visual reasoning capabilities has garnered significant attention from both industry and academia for its potential to drive transformative advancements.

Researchers have explored two primary categories of methods to enhance visual reasoning capabilities: (1) neural-symbolic methods [32–36], which integrate symbolic reasoning with neural networks to improve interpretability and modularity, and (2) Supervised Fine-Tuning (SFT) based on vision-language models (VLMs) [37, 38], which utilize end-to-end training to strengthen reasoning abilities.

* Equal contribution. † Project leader. ✉ Corresponding author: shanghang@pku.edu.cn.

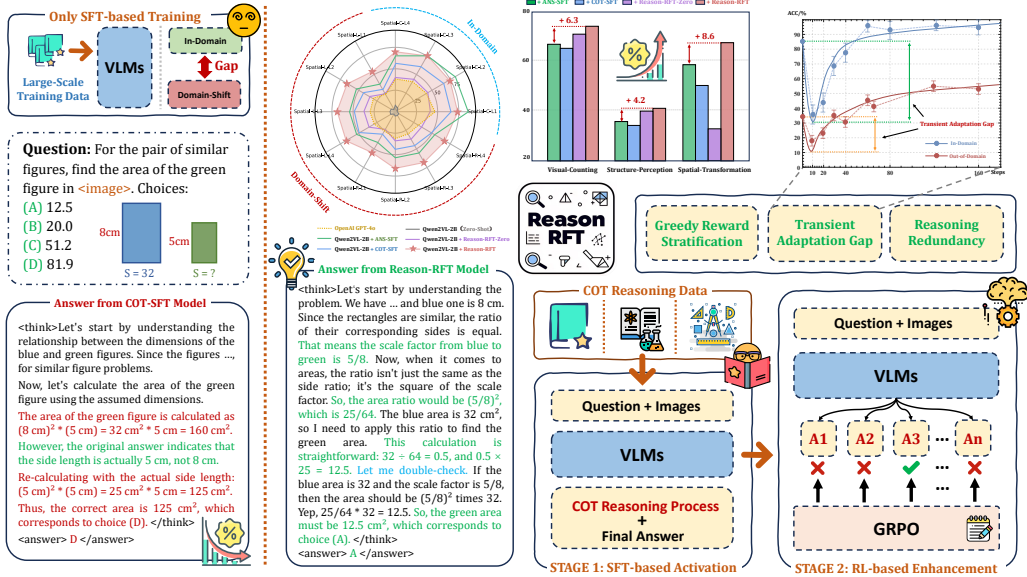


Figure 1: **Overview of Reason-RFT.** Compared to traditional SFT-based methods, our proposed Reason-RFT framework demonstrates superior generalization in visual reasoning tasks, excelling in reasoning improvement, domain shift adaptability, and data efficiency.

However, both approaches face significant limitations. Neural-symbolic methods are hindered by high complexity and a strong reliance on program generation, while SFT is constrained by its dependence on high-quality Chain-of-Thought (CoT) annotated data and meticulously designed data mixing strategies, leading to issues such as overfitting, cognitive rigidity, and limited adaptability to domain shift. These challenges reduce their effectiveness in real-world applications.

Recent advances such as GPT-o1 [2], DeepSeek-R1 [39], and Kimi-1.5 [40] show that reinforcement learning (RL) during post-training enhances reasoning in coding and mathematics. RL offers a dynamic alternative to SFT by enabling exploration and feedback-driven optimization, which can improve performance with limited labeled data. However, pure RL methods often lack robustness to domain shifts—such as changes in visual appearance or configuration, limiting their generalization capacity in real-world visual reasoning scenarios.

To address this, we propose **Reason-RFT**, the first two-stage reinforcement fine-tuning framework designed to enhance generalization in visual reasoning tasks. First, we employ SFT with CoT reasoning to activate the model’s potential reasoning capabilities, using a high-quality domain-specific visual reasoning dataset tailored to stimulate related reasoning abilities. Subsequently, we further enhance reasoning potential through Group Relative Policy Optimization (GRPO), demonstrating that *Reason-RFT* improves robustness under distribution shifts by enhancing the model’s reasoning capabilities. To evaluate its effectiveness, we constructed a high-quality dataset covering visual counting, structure perception, and spatial transformation, serving as a benchmark for evaluating three core capabilities of visual reasoning. Extensive experiments highlight three key advantages of *Reason-RFT*: (1) **Performance Improvement**: It achieves strong results on visual reasoning tasks, including visual counting, structure perception, and spatial transformation, outperforming mainstream VLMs; (2) **Enhanced Generalization**: It consistently exceeds both SFT-only and RL-only baselines under domain shift conditions, as demonstrated through comprehensive evaluations; (3) **Data Efficiency**: It reaches over 90% of the SFT-only performance while using less than 5% of the data. These results underscore the effectiveness and efficiency of *Reason-RFT*, establishing it as a robust framework for advancing visual reasoning. Our main contributions are summarized as follows.

- We introduce **Reason-RFT**, a two-stage reinforcement fine-tuning framework that significantly enhances the visual reasoning capabilities of VLMs by effectively combining the complementary strengths of SFT-based and RL-based methods.
- We provide a systematic analysis of SFT-based and RL-based paradigms on visual reasoning tasks, identifying the limitations of SFT and the advantages of RL in improving reasoning ability, handling domain shifts, and achieving data-efficient learning.

- We reconstruct a comprehensive dataset spanning three core domains: visual counting, structure perception, and spatial transformation, serving as a benchmark for evaluating visual cognition, geometric understanding, and spatial generalization.
- Extensive experiments validate the proposed framework, demonstrating its practicality and effectiveness, and providing a new perspective for reinforcement-driven multi-modal training.

2 Related Work

Visual Reasoning Visual reasoning is a core challenge in advancing AGI, requiring models to perform complex cognitive tasks grounded in visual perception [1, 41–50]. It underpins a wide range of applications, including visual counting [1, 51], geometric problem-solving [41, 52–55], visual transformation reasoning [56, 57], scientific analysis [58, 59], and robotic task planning [17, 60, 61]. Traditional approaches rely on program generation [36, 62, 63] or neural-symbolic reasoning [32–35], while recent advances in VLMs leverage large language models (LLMs) to enhance reasoning capabilities. For instance, LLaVA-CoT [37] employs multi-stage SFT with CoT prompting [64], and Insight-V [65] integrates SFT with RL. DeepSeek-R1-Zero [66] further introduces a rule-guided RL framework that substantially improves reasoning performance. Building upon the DeepSeek-R1 [66], our work provides a comparative analysis of SFT-based and RL-based paradigms, demonstrating the advantages of R1-style methods in enhancing visual reasoning.

Post-Training Post-Training is a crucial phase for enhancing the performance of LLMs and VLMs, bridging pre-trained models and their real-world applications [67–70]. It primarily involves two methodologies: *SFT* [71, 72] and *RL* [73–77]. SFT adapts pre-trained models to specific tasks using task-oriented datasets, often formatted as instructions. Research like FLAN [78] highlights the importance of diverse instruction-tuning datasets for improving zero-shot performance, while iterative processes, such as Llama 3.1’s six-round strategy [79], integrate rejection sampling, synthetic data, and human annotations. RL aligns models with human preferences or task-specific goals through feedback mechanisms. Reinforcement Learning from Human Feedback (RLHF) [74] refines models using human preference data, as seen in Llama 3.1 [79] and Nemotron-4 [80], which use reward modeling techniques like DPO [81] and RPO [80]. For example, TÜLU3 [82] employs length-normalized DPO, while DeepSeek-V3 [83] combines rule-based and model-based reward systems. Recently, DeepSeek-R1 [66] achieved significant text reasoning improvements through pure RL [84]. Our work first adapts R1 methodologies to VLMs, enhancing visual reasoning, and systematically compares SFT-based and RL-based paradigms in visual reasoning tasks.

3 Methodology

In this section, we introduce ***Reason-RFT***, a novel two-stage training strategy to enhance the reasoning capabilities of VLMs in complex visual reasoning tasks. As shown in Fig. 2, the framework comprises two stages: (1) *SFT-based Visual Reasoning Activation*, which uses SFT with high-quality CoT reasoning data to activate the model’s domain-specific reasoning capabilities, and (2) *RL-based Reasoning Enhancement*, which employs the GRPO algorithm with rule-based rewards to further push the upper limits of the model’s reasoning potential.

3.1 STAGE 1: SFT-based Reasoning Activation

In the initial stage, we employ SFT on a structured visual reasoning dataset containing step-by-step reasoning processes. This stage trains the model to decompose complex tasks into logical steps. Each sample is represented as (x, q, r, a) , where x denotes the input images, q is the question, r is the reasoning steps, and a is the final answer. The training objective maximizes the likelihood of generating both r and a given (x, q) :

$$\mathcal{L}_{\text{SFT}} = -\mathbb{E}_{(x, q, r, a) \sim \mathcal{D}} \sum_{t=1}^T \log \pi_{\theta}(y_t | x, q, y_{<t}), \quad (1)$$

where \mathcal{D} denotes the dataset, y represents the concatenated sequence of r and a , and π_{θ} denotes the model’s token distribution. The resulting model π_{CoT} is used to initialize the subsequent stage, providing a stable foundation for RL-based reasoning enhancement.

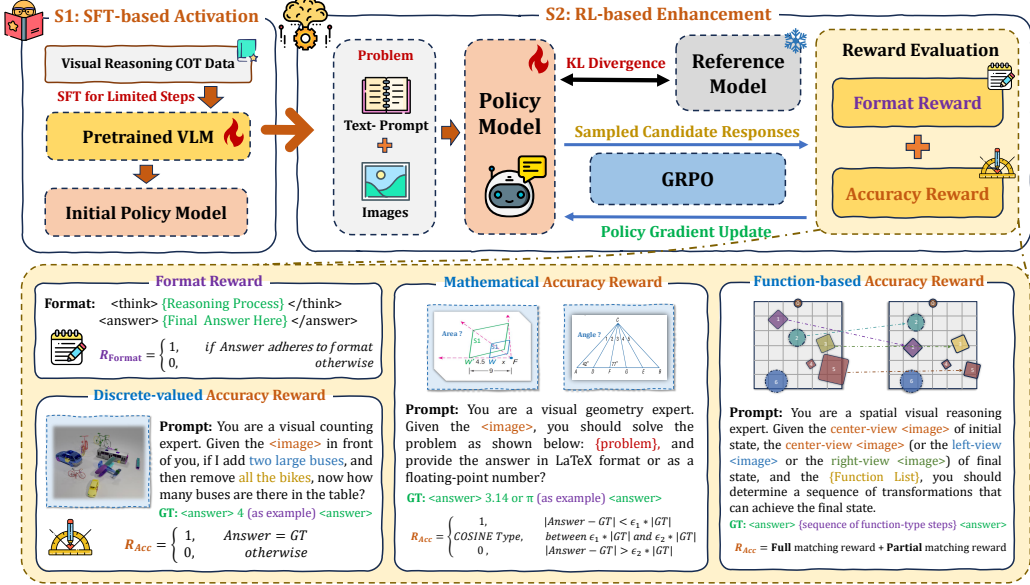


Figure 2: **Framework of Reason-RFT**. Reason-RFT adopts a two-stage training paradigm for visual reasoning. The first stage applies SFT with CoT reasoning to establish strong task-specific priors. In the second stage, GRPO is employed to further enhance reasoning capability and generalization.

3.2 STAGE 2: RL-based Reasoning Enhancement

In the second stage, we refine π_{CoT} using GRPO, leveraging RL for its efficiency and scalability. Unlike Proximal Policy Optimization (PPO), which requires a computationally expensive value network, GRPO calculates relative advantages by comparing rewards within a group of sampled actions, reducing computational overhead and simplifying optimization. This makes GRPO particularly suitable for visual reasoning tasks.

Sampling Action Groups For each input state $s = (x, q)$, GRPO samples a group of actions $\{a_1, a_2, \dots, a_G\}$ from the current policy π_θ , initialized from π_{CoT} . The sampling process is:

$$a_i \sim \pi_\theta(a | x, q), \quad \text{for } i = 1, 2, \dots, G. \quad (2)$$

This strategy ensures diverse responses, promoting exploration and preventing premature convergence.

Reward Evaluation. Each sampled action a_i receives a reward $R(a_i)$ based on verifiable criteria, yielding a reward set $\{r_1, r_2, \dots, r_G\}$. For visual reasoning tasks, the reward $R(a_i)$ is composed of a format reward $R_{\text{format}}(a_i)$, which enforces structured outputs, and an accuracy reward $R_{\text{acc}}(a_i)$, which measures correctness. This formulation balances structural alignment and factual precision in reasoning. The reward function is defined as:

$$R(a_i) = R_{\text{format}}(a_i) + R_{\text{acc}}(a_i). \quad (3)$$

Policy Update with Relative Advantage Rewards are normalized within the sampled group to compute relative advantages $\{A_1, A_2, \dots, A_G\}$, defined as:

$$A_i = \frac{r_i - \text{mean}\{r_1, r_2, \dots, r_G\}}{\text{std}\{r_1, r_2, \dots, r_G\}}. \quad (4)$$

Based on these advantages, the policy is updated to reinforce actions with positive advantages and reduce the probability of less effective ones. To maintain training stability, the update is constrained by minimizing the KL divergence between the updated and reference policies.

3.3 Reward Design for Visual Reasoning Tasks

For the diverse requirements of visual reasoning tasks, including visual counting, structure perception, and spatial transformation, our reward design integrates two essential components: *format reward* and *accuracy reward*. The format reward is uniformly applied across all tasks, ensuring that the

model strictly adheres to a structured response format for consistency. For the accuracy reward, we carefully tailor the design to the specific characteristics of each task, as shown in Fig. 2, creating task-specific reward mechanisms to evaluate the correctness of the model’s responses.

Format Reward This component ensures structured and interpretable responses by requiring the model to adhere to a predefined template: reasoning within `<think>` and `</think>` and the final answer within `<answer>` and `</answer>`. A reward of 1 is only given for strict adherence.

Accuracy Reward This component evaluates the correctness of the model’s responses, ensuring alignment with ground truth across diverse visual reasoning tasks. To address task diversity, we design tailored reward mechanisms for discrete-valued, mathematical, and function-based problems. Each mechanism is crafted to handle the unique characteristics of its problem category, enabling precise and fair evaluation. Below, we introduce the three reward forms.

- **Discrete-valued Type** This reward type applies to visual counting and structure perception tasks, where answers are discrete values (e.g., multiple-choice or integer-based responses). The accuracy reward $R_{\text{acc}}(a_i)$ is defined as:

$$R_{\text{acc}}(a_i) = \begin{cases} 1, & \text{if } a_{\text{pred}} = a_{\text{gt}} \\ 0, & \text{otherwise,} \end{cases} \quad (5)$$

where a_{pred} is the predicted answer and a_{gt} is the ground truth. This discrete reward penalizes deviations from ground truth, ensuring precision in tasks requiring unambiguous answers.

- **Mathematical Type** This reward type is designed for structure perception tasks involving numerical answers, such as floating-point values or LaTeX-formatted expressions. It uses a tolerance-based evaluation to account for minor numerical deviations, which is defined as:

$$R_{\text{acc}}(a_i) = \frac{1}{2} \left[\cos \left(\pi \times \frac{|a_{\text{pred}} - a_{\text{gt}}| - \epsilon_1 \times |a_{\text{gt}}|}{(\epsilon_2 - \epsilon_1) \times |a_{\text{gt}}|} \right) + 1 \right], \quad (6)$$

where a_{pred} is the predicted answer, a_{gt} is the ground truth, ϵ_1 is the tolerance threshold for an exact match (e.g., 0.05), and ϵ_2 is the upper bound for partial rewards (e.g., 0.20). If $|a_{\text{pred}} - a_{\text{gt}}| < \epsilon_1 \times |a_{\text{gt}}|$, the reward is 1 (exact match); if $|a_{\text{pred}} - a_{\text{gt}}| > \epsilon_2 \times |a_{\text{gt}}|$, the reward is 0 (incorrect). This formulation ensures smooth transitions between full and partial rewards, enabling fair evaluation of numerical accuracy.

- **Function-based Type** This reward type is designed for spatial transformation tasks requiring a sequence of transformation functions. The accuracy reward $R_{\text{acc}}(a_i)$ evaluates the alignment between the predicted sequence T_{pred} and the ground truth T_{gt} , computed as:

$$R_{\text{acc}}(a_i) = \frac{\text{len}(T_{\text{pred}}^{f+o+v}) + \alpha \cdot \text{len}(T_{\text{pred}}^{f+o/v}) + \beta \cdot \text{len}(T_{\text{pred}}^f)}{\max(\text{len}(T_{\text{pred}}), \text{len}(T_{\text{gt}}))}, \quad (7)$$

where T_{pred}^{f+o+v} is the subset of transformation steps with complete matches (w/ function, object, and value), $T_{\text{pred}}^{f+o/v}$ are the subsets with partial and only-function matches (w/ function and object, or w/ function and value), T_{pred}^f is the subset with only-function matches. α and β are the weighting coefficients for partial matches. This formulation ensures nuanced evaluation for flexible adjustment of partial match contributions.

4 Experiments

We design experiments to investigate the following key research questions:

- **RQ1:** How effective is *Reason-RFT* in reasoning, generalization, and data efficiency?
- **RQ2:** Why is the STAGE 1 of SFT with CoT reasoning necessary?
- **RQ3:** Why is the STAGE 2 of reinforcement fine-tuning necessary?
- **RQ4:** How does reward design affect *Reason-RFT*’s performance?
- **RQ5:** What training dynamics emerge during reinforcement fine-tuning, and how do they shape the reasoning behavior of *Reason-RFT*?

4.1 Experimental Details

Datasets In this paper, we comprehensively evaluate the visual reasoning capabilities of our method by leveraging six existing datasets, enhanced through subtask categorization, error-prone data filtering, and dataset restructuring. Detailed protocols for data filtering and restructuring are provided in Sec. A. Specifically, we define three task categories as follows.

- **Visual Counting** is a multimodal reasoning task evaluating the integration of linguistic, visual, and mathematical skills by solving arithmetic problems in 3D block-based scenes. Specifically, we filtered and corrected 35K samples from CLEVR-Math [1] for training and 1K test samples for in-domain (ID) evaluation. To assess generalization under domain-shift (DS), we constructed 1K new samples using 3D assets from Super-CLEVR [51], including two subsets: direct arithmetic (DS-D) and mixed arithmetic (DS-M). Refer to the Appendix Sec. A.1 for details.
- **Structure Perception** is a structural reasoning task requiring models to analyze relationships in geometries, imaging structures, chart layouts, and architectural designs. We filtered 4.5K training samples and 820 ID test samples from Geo170K [52] and Math360K [55], along with 800 samples from Geometry3K [85] to evaluate DS adaptability. See the Appendix Sec. A.2.
- **Spatial Transformation** is a spatial-visual reasoning task requiring models to infer single- or multi-step transformations by analyzing initial and final states of 3D scenes from multiple perspectives (*e.g.*, center, left, right). We generated 100K samples using TRANCE [56], covering four difficulty levels, and selected 60K for training and 6K for testing through a specific filtering process. For DS evaluation, identical scenes are rendered from left/right viewpoints (DS-L/R) to test perspective-change robustness. Details can be found in the Appendix Sec. A.3.

Evaluation Metrics We use accuracy-rate (Acc) as the primary metric [86]. For numerical answers, correctness is verified by mathematical equivalence to the ground truth. For multiple-choice questions, we perform a string match. For function-type sequences, we use stepwise multi-level evaluation.

Implementation Details We utilize Qwen2-VL-2B and Qwen2-VL-7B [87] as the backbone models for our experiments. Our implementation is built on the open-source frameworks Open-R1 [88] and vLLM [89], ensuring reproducibility and scalability. All experiments were conducted on a cluster of servers, each equipped with $8 \times$ A800 GPUs. For further details, see the Appendix Sec. B.

Training Paradigms and Baselines To assess the performance and generalization of different training strategies, we compare: (1) SFT-based methods—ANS-SFT, which fine-tunes on answer generation, and CoT-SFT, which uses supervised learning with CoT reasoning; and (2) RL-based methods—Reason-RFT-Zero, which applies RL without reasoning activation stage, and Reason-RFT, which uses limited CoT data for reasoning activation before RL training. For comprehensive experiments, we use Qwen2-VL-Instruct [87] as the base model (both 2B and 7B variants). In addition, we also select the most advanced open-source models [90–94] and the proprietary models [95, 96] as baselines to evaluate the performance of different paradigms.

4.2 Overall Evaluation of Reason-RFT Framework (RQ1)

To evaluate Reason-RFT, we evaluate Reason-RFT using 2B- and 7B-parameter models on three visual reasoning tasks. The results are summarized as follows.

Strong reasoning performance across ID tasks. As shown in Tab. 1, Reason-RFT achieves performance comparable to or better than both SFT- and RL-based methods across all tasks. In *visual counting*, Reason-RFT-Zero achieves the best performance among all models in the 7B setting. In *structure perception*, Reason-RFT outperforms most open-source and proprietary baselines in the 7B setting and remains competitive with top models such as InternVL-2.5-8B [92]. In *spatial transformation*, Reason-RFT matches or exceeds SFT-based methods while consistently outperforming all baselines. These results demonstrate that Reason-RFT effectively integrates the strengths of both SFT and RL in structured reasoning tasks.

Superior generalization under DS. Under DS settings, Reason-RFT shows substantial gains over both traditional baselines and alternative training paradigms. In *visual counting*, it outperforms ANS-SFT by 10.95% (2B) and 13.93% (7B). In *structure perception*, Reason-RFT achieves the highest performance in the 2B model, with an 6.93% gain over CoT-SFT, and remains highly competitive in

Table 1: **Results on three visual reasoning tasks.** The best results among different training paradigms are highlighted in **bold**, while the second-best results are underlined. “ID” denotes in-domain test data, and “DS” denotes domain-shift test data.

Method	Visual Counting				Structure Perception			Spatial Transformation			
	ID	DS-D	DS-M	AVG	ID	DS	AVG	ID	DS-L	DS-R	AVG
Proprietary Models											
GPT-4o-2024-08-06 [95]	68.10	42.54	9.60	40.08	50.18	43.49	46.83	42.55	28.67	29.76	35.88
Gemini-1.5-Pro [96]	61.80	41.20	26.40	43.13	50.12	48.38	49.45	26.22	18.76	19.88	22.77
Open-Source Models											
Qwen2.5-VL-3B-Inst. [90]	75.90	50.93	4.40	43.74	36.75	37.44	37.09	8.57	8.26	8.31	8.42
Phi-3.5-Vision-4B-Inst. [91]	21.40	18.27	6.00	15.22	36.83	50.25	43.54	7.42	2.45	4.02	5.33
Qwen2.5-VL-7B-Inst. [90]	74.60	46.00	2.80	41.13	44.00	45.61	44.80	19.63	13.12	13.42	16.45
InternVL-2.5-SB [92]	93.50	46.13	2.80	47.48	63.00	47.32	51.60	7.19	6.62	6.63	6.91
Llama-3.2-11B-Vision [93]	10.30	9.60	9.20	9.70	13.75	20.85	17.30	8.22	8.40	9.03	8.47
Pixtral-12B [94]	42.60	25.33	15.60	27.84	30.38	36.09	33.23	7.35	5.03	5.22	6.42
Qwen2VL-2B-Instruct											
Zero-Shot	82.40	42.67	0.00	41.69	25.86	20.63	23.25	3.78	4.60	4.67	4.35
+ ANS-SFT	96.20	51.07	5.20	50.82	51.34	22.50	36.92	77.39	49.24	<u>50.33</u>	<u>58.99</u>
+ CoT-SFT	85.50	49.73	36.80	<u>57.34</u>	43.05	25.25	34.15	64.37	43.19	42.86	<u>50.14</u>
+ Reason-RFT-Zero	98.40	<u>58.00</u>	5.20	53.87	47.68	<u>32.50</u>	<u>40.09</u>	42.13	34.07	33.41	33.74
+ Reason-RFT	96.80	60.00	<u>28.40</u>	61.77	<u>49.03</u>	<u>33.13</u>	41.08	74.61	64.05	64.08	67.58
Qwen2VL-7B-Instruct											
Zero-Shot	<u>98.60</u>	54.53	4.80	52.64	43.30	43.88	43.59	13.53	12.72	12.78	13.01
+ ANS-SFT	95.00	42.53	8.00	48.51	51.34	25.38	38.36	82.19	54.29	<u>54.83</u>	<u>63.77</u>
+ CoT-SFT	87.30	45.33	<u>33.60</u>	55.41	50.49	33.00	41.75	<u>81.31</u>	47.90	47.80	59.00
+ Reason-RFT-Zero	99.40	63.60	21.20	<u>61.40</u>	<u>55.00</u>	54.75	54.88	67.67	57.20	56.15	60.34
+ Reason-RFT	95.60	<u>56.13</u>	35.60	62.44	<u>59.27</u>	<u>49.25</u>	<u>54.26</u>	79.97	59.36	58.61	65.98

the 7B model. Most notably, in the *spatial transformation* task, the 2B Reason-RFT model surpasses GPT-4o [95] by 31.7%, showcasing remarkable generalization under DS.

High training efficiency. To evaluate data efficiency during training, we train all methods on the *spatial transformation* task and monitor intermediate ID and DS performance (Fig. 3). Additional results for *visual counting* and *structure perception* are provided in Appendix Sec. C. In the 2B model, Reason-RFT achieves 70% of the final performance of Reason-RFT-Zero using only 3% of the training data (1,600 samples), and reaches 82.5% with 9% of the data. In the 7B model, it achieves over 92% of Reason-RFT-Zero’s performance using just 3% of the data. These results confirm that Reason-RFT exhibits strong training efficiency in both ID and DS scenarios. The data-efficient nature of Reason-RFT renders it particularly effective for few-shot learning, offering significant potential for applications where labeled data is limited.

4.3 Effect of STAGE 1 on Initialization (RQ2)

To investigate the role of CoT-SFT in initialization, we compare four baselines across three tasks. The results in Tab. 1 reveal the following: (1) **Consistent performance gains from CoT-SFT.** Across all three tasks and both 2B and 7B model scales, Reason-RFT consistently outperforms Reason-RFT-Zero following stage 1 reasoning activation. This improvement is particularly notable when the model is small and the task involves complex output structures. For example, in the *spatial transformation* task—which requires function-like serialized outputs—the 2B Reason-RFT model surpasses Reason-RFT-Zero by 33.84%. (2) **Smaller models benefit more from CoT-SFT priors.** In the *visual counting* task under the DS-M setting, the 2B model with CoT-SFT outperforms Reason-RFT-Zero by 31.6%.

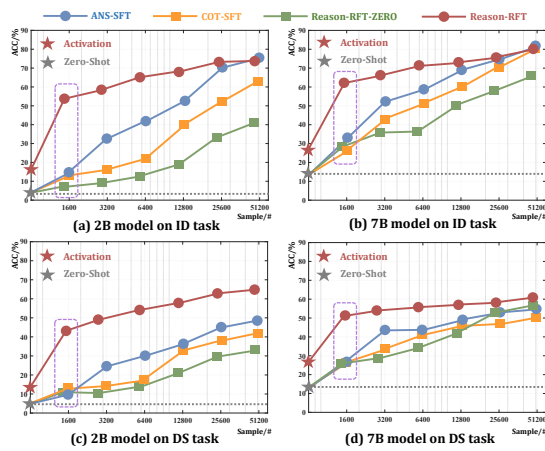


Figure 3: Results of different methods and model sizes on *spatial transformation* task across training.

Although the gap narrows in the 7B model, CoT-SFT still yields substantial gains. This indicates that pure RL-based methods struggle to adapt from direct arithmetic to mixed arithmetic reasoning under DS, whereas CoT-SFT provides effective inductive priors for such adaptation. Moreover, under the same amount of CoT-SFT data, the 2B model still underperforms its 7B counterpart, highlighting the increased reliance of smaller models on CoT-SFT for acquiring reasoning capabilities.

4.4 Effect of STAGE 2 on Generalization (RQ3)

To evaluate the impact of RL in stage 2, we compare the generalization performance of CoT-SFT and Reason-RFT across three visual reasoning tasks under DS. As shown in Tab. 1 and Fig. 4, the results reveal the following: **Reinforcement fine-tuning improves generalization beyond CoT-SFT**. Across all domain-shift settings, Reason-RFT consistently outperforms CoT-SFT, demonstrating that reinforcement learning significantly enhances model robustness. For instance, in the *visual counting* task, the 7B Reason-RFT achieves a combined DS-D and DS-M score 12.8% higher than CoT-SFT. The improvement is even more pronounced in structure-sensitive tasks such as *spatial transformation*, where the 2B Reason-RFT exceeds CoT-SFT by 21.04% on average across DS-L and DS-R. These results indicate that CoT-SFT alone yields limited generalization, while reinforcement fine-tuning enables better adaptation to compositional and layout-dependent variations.

4.5 Exploration on Reward Design (RQ4)

Format Reward. In DeepSeek-R1 [39], the format reward enforces the use of `<think>` and `<answer>` tokens to structure reasoning in textual tasks. To better support visual reasoning, we extend this with `<summary>` and `<caption>` tokens to incorporate visual observations via caption-style prompts. As shown in Tab. 2, this improves Reason-RFT-Zero but has limited effect on Reason-RFT. We attribute this to Reason-RFT’s prior CoT supervision, which likely helps it internalize caption-like structures in stage 1, reducing the benefit of explicit tags. In contrast, Reason-RFT-Zero benefits more from such structural cues, indicating greater sensitivity to format-level guidance.

Accuracy Reward. We explore accuracy reward design in the *spatial transformation* task, which requires predicting transformation sequences in a structured format. The formulation in Eq. 7 introduces coefficients α and β to control tolerance for partial matches. We test three settings: (1) $\alpha = 0, \beta = 0$ (exact match only), (2) $\alpha = 0.50, \beta = 0.25$ (partial credit), and (3) $\alpha = -0.25, \beta = -0.50$ (penalized partial matches). Results on 2B and 7B models (Tab. 3) show that: (1) partial credit improves ID performance but harms generalization, suggesting “soft rewards” reduce robustness; (2) penalizing partial matches improves generalization under domain shift, indicating “hard rewards” better support serialized reasoning.

4.6 Training Dynamics and Reasoning Behavior Analysis (RQ5)

Greedy Reward Stratification. This phenomenon captures the model’s tendency, particularly in Reason-RFT-Zero, to prioritize easier-to-optimize rewards (e.g., format reward) before addressing more challenging objectives (e.g., accuracy reward). As shown in Fig. 5, the reasoning token length initially drops, then gradually increases and stabilizes. This dynamic correlates with the format

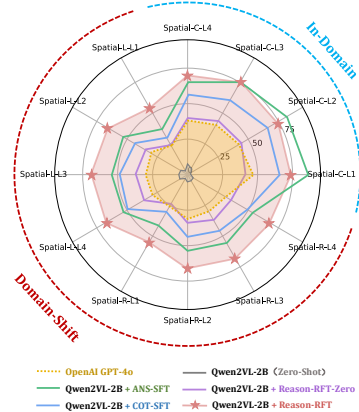


Figure 4: Results of DS v.s. ID on *spatial transformation* task.

Table 2: Results of different format reward strategies on the *spatial transformation* task.

Setting	ID	DS-L	DS-R	AVG
Qwen2VL-2B-Instruct				
Reason-RFT-Zero	42.13	34.07	33.41	33.74
+ visual tokens	42.01	36.05	35.97	38.01
Reason-RFT	74.61	64.05	64.08	69.33
+ visual tokens	71.99	60.13	59.87	65.99
Qwen2VL-7B-Instruct				
Reason-RFT-Zero	67.67	57.2	56.15	62.17
+ visual tokens	70.28	59.52	57.01	64.27
Reason-RFT	79.97	59.36	58.61	69.48
+ visual tokens	79.85	58.71	57.98	69.09

Table 3: Results of different accuracy reward strategies on the *spatial transformation* task.

Setting	α	β	ID	DS-L	DS-R	AVG
Qwen2VL-2B-Instruct						
Baseline	0	0	74.61	64.05	64.08	69.33
(a)	0.50	0.25	79.18	56.36	55.45	67.54
(b)	-0.25	-0.50	73.69	64.41	64.72	69.13
Qwen2VL-7B-Instruct						
Baseline	0	0	79.97	59.36	58.61	69.48
(a)	0.50	0.25	80.89	53.20	52.61	66.90
(b)	-0.25	-0.50	75.03	64.83	63.18	69.52

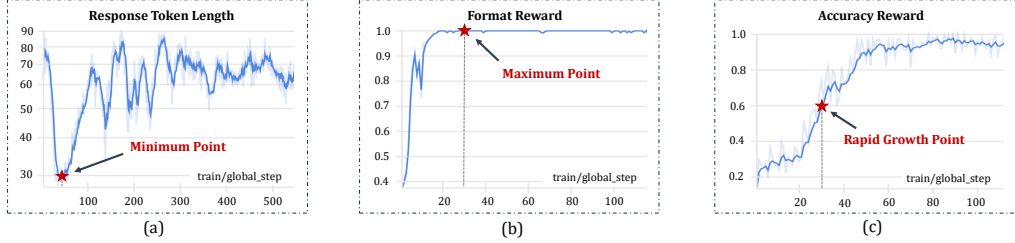


Figure 5: **Analysis of Greedy Reward Stratification.** The model’s reasoning token length first decreases, then gradually rises and stabilizes during Reason-RFT-Zero training. The peak of the format reward coincides with the accuracy reward’s rapid growth phase.

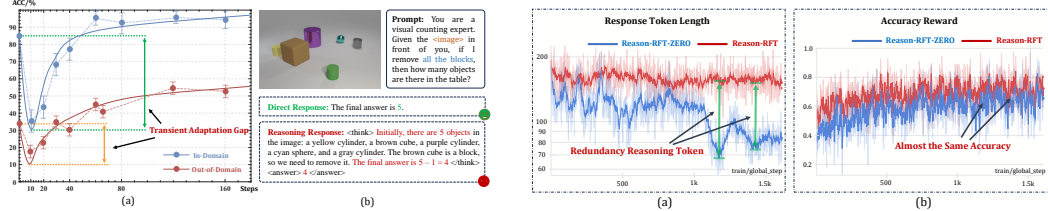


Figure 6: **Illustration of the Transient Adaptation Gap.** (a) shows a sharp drop and recovery in both ID and DS test performances within the early training steps. (b) shows a case study of the prediction result on early step.

Figure 7: **Analysis of Reasoning Redundancy.** (a) shows the reasoning token length curves for Reason-RFT-Zero and Reason-RFT during training. (b) displays their accuracy reward, with both paradigms converging to similar accuracy rate.

reward quickly reaching a plateau, followed by a sharp rise in the accuracy reward. We infer that the model initially simplifies its outputs to adapt rapidly to structured format expectations, and only later allocates learning capacity to improve reasoning correctness.

Transient Adaptation Gap. This refers to a temporary performance degradation observed in the early training phase of Reason-RFT-Zero. When the model shifts from directly predicting answers to producing structured reasoning traces, it experiences a brief adaptation bottleneck—marked by a sharp decline and gradual recovery in accuracy. Fig. 6 (a) illustrates this drop within the first 100 steps on the *visual counting* task under both ID and DS settings. A case analysis in Fig. 6 (b) further reveals that forcing structured reasoning prematurely may lead to incorrect outputs, highlighting the sensitivity of early-stage training to reasoning format constraints.

Reasoning Redundancy. This phenomenon concerns the discrepancy in reasoning token length between models trained with and without CoT activation. In the *structure perception* task, Reason-RFT and Reason-RFT-Zero attain similar accuracy, yet the former generates significantly longer reasoning traces (Fig. 7). This likely stems from Reason-RFT’s use of CoT data distilled from advanced models (e.g., GPT-4o), which encourages verbose reasoning during stage 1. In the absence of penalties or length control in reinforcement fine-tuning, such verbosity persists. By contrast, Reason-RFT-Zero converges to more concise reasoning through reward-driven exploration. We hypothesize that these longer chains in Reason-RFT may introduce unnecessary computational overhead or reflect overthinking relative to task complexity.

5 Conclusion

In this paper, we propose **Reason-RFT**, a novel reinforcement fine-tuning framework that enhances the generalization capabilities of visual reasoning models. By integrating SFT with CoT reasoning activation data and GRPO-based reinforcement learning, **Reason-RFT** effectively mitigates key challenges such as overfitting and cognitive rigidity, thereby improving cross-domain transferability and real-world applicability. To support systematic evaluation, we reconstruct a comprehensive dataset covering visual counting, structure perception, and spatial transformation tasks, establishing a robust benchmark for assessing model performance across diverse scenarios. Extensive experiments demonstrate the effectiveness of **Reason-RFT**, providing valuable insights for advancing visual reasoning research and introducing a new paradigm in multimodal learning.

Acknowledgments

This work was supported by the National Natural Science Foundation of China (62476011), and the National Science and Technology Major Project (No. 2022ZD0117800).

References

- [1] Adam Dahlgren Lindström and Savitha Sam Abraham. Clevr-math: A dataset for compositional language, visual and mathematical reasoning. *arXiv preprint arXiv:2208.05358*, 2022.
- [2] OpenAI. Learning to reason with llms. <https://openai.com/index/learning-to-reason-with-llms/>, 2024. Accessed: 2025-03-02.
- [3] Maria MP Petrou and Costas Petrou. *Image processing: the fundamentals*. John Wiley & Sons, 2010.
- [4] Huajie Tan, Guoqing Xiang, Xiaodong Xie, and Huizhu Jia. Joint frame-level and block-level rate-perception optimized preprocessing for video coding. In *Proceedings of the 6th ACM International Conference on Multimedia in Asia*, pages 1–1, 2024.
- [5] Qizhe Zhang, Mengzhen Liu, Lichen Li, Ming Lu, Yuan Zhang, Junwen Pan, Qi She, and Shanghang Zhang. Beyond attention or similarity: Maximizing conditional diversity for token pruning in mllms. *arXiv preprint arXiv:2506.10967*, 2025.
- [6] Yuheng Ji, Yue Liu, Zhicheng Zhang, Zhao Zhang, Yuting Zhao, Gang Zhou, Xingwei Zhang, Xinwang Liu, and Xiaolong Zheng. Advlora: Adversarial low-rank adaptation of vision-language models. *arXiv preprint arXiv:2404.13425*, 2024.
- [7] Yuheng Ji, Yue Liu, Zhicheng Zhang, Zhao Zhang, Yuting Zhao, Xiaoshuai Hao, Gang Zhou, Xingwei Zhang, and Xiaolong Zheng. Enhancing adversarial robustness of vision-language models through low-rank adaptation. In *Proceedings of the 2025 International Conference on Multimedia Retrieval*, pages 550–559, 2025.
- [8] Yuheng Ji, Xingwei Zhang, Gang Zhou, Xiaolong Zheng, and Daniel Dajun Zeng. Learning hash subspace from large-scale multi-modal pre-training: A clip-based cross-modal hashing framework. In *China Conference on Command and Control*, pages 514–526. Springer, 2023.
- [9] Huaihai Lyu, Chaofan Chen, Yuheng Ji, and Changsheng Xu. Egoprompt: Prompt pool learning for egocentric action recognition. *arXiv preprint arXiv:2508.03266*, 2025.
- [10] Jianan Mu, Huajie Tan, Shuai Chen, Min Cai, Jing Ye, Huawei Li, and Xiaowei Li. Configurable and high-level pipelined lattice-based post quantum cryptography hardware accelerator design. In *2023 IEEE 32nd Asian Test Symposium (ATS)*, pages 1–6. IEEE, 2023.
- [11] Jianan Mu, Huajie Tan, Jiawen Wu, Haotian Lu, Chip-Hong Chang, Shuai Chen, Shengwen Liang, Jing Ye, Huawei Li, and Xiaowei Li. Energy-efficient ntt design with one-bank sram and 2-d pe array. In *2023 Design, Automation & Test in Europe Conference & Exhibition (DATE)*, pages 1–2. IEEE, 2023.
- [12] Songran Bai, Yuheng Ji, Yue Liu, Xingwei Zhang, Xiaolong Zheng, and Daniel Dajun Zeng. Alleviating performance disparity in adversarial spatiotemporal graph learning under zero-inflated distribution. In *Proceedings of the AAAI Conference on Artificial Intelligence*, volume 39, pages 11436–11444, 2025.
- [13] Marius Cordts, Mohamed Omran, Sebastian Ramos, Timo Rehfeld, Markus Enzweiler, Rodrigo Benenson, Uwe Franke, Stefan Roth, and Bernt Schiele. The cityscapes dataset for semantic urban scene understanding. In *IEEE conference on computer vision and pattern recognition*, pages 3213–3223, 2016.
- [14] Jihan Yang, Shusheng Yang, Anjali W Gupta, Rilyn Han, Li Fei-Fei, and Saining Xie. Thinking in space: How multimodal large language models see, remember, and recall spaces. *arXiv preprint arXiv:2412.14171*, 2024.
- [15] Li-Ming Zhan, Bo Liu, Lu Fan, Jiaxin Chen, and Xiao-Ming Wu. Medical visual question answering via conditional reasoning. In *ACM International Conference on Multimedia*, pages 2345–2354, 2020.

- [16] Jiazen Pan, Che Liu, Junde Wu, Fenglin Liu, Jiayuan Zhu, Hongwei Bran Li, Chen Chen, Cheng Ouyang, and Daniel Rueckert. Medvilm-r1: Incentivizing medical reasoning capability of vision-language models (vlms) via reinforcement learning. *arXiv preprint arXiv:2502.19634*, 2025.
- [17] Yuheng Ji, Huajie Tan, Jiayu Shi, Xiaoshuai Hao, Yuan Zhang, Hengyuan Zhang, Pengwei Wang, Mengdi Zhao, Yao Mu, Pengju An, et al. Robobrain: A unified brain model for robotic manipulation from abstract to concrete. In *Proceedings of the Computer Vision and Pattern Recognition Conference*, pages 1724–1734, 2025.
- [18] BAAI RoboBrain Team, Mingyu Cao, Huajie Tan, Yuheng Ji, Minglan Lin, Zhiyu Li, Zhou Cao, Pengwei Wang, Enshen Zhou, Yi Han, et al. Robobrain 2.0 technical report. *arXiv preprint arXiv:2507.02029*, 2025.
- [19] Jiaming Liu, Mengzhen Liu, Zhenyu Wang, Lily Lee, Kaichen Zhou, Pengju An, Senqiao Yang, Renrui Zhang, Yandong Guo, and Shanghang Zhang. Robomamba: Multimodal state space model for efficient robot reasoning and manipulation. *arXiv e-prints*, pages arXiv–2406, 2024.
- [20] Huajie Tan, Xiaoshuai Hao, Cheng Chi, Minglan Lin, Yaoxu Lyu, Mingyu Cao, Dong Liang, Zhuo Chen, Mengsi Lyu, Cheng Peng, et al. Roboos: A hierarchical embodied framework for cross-embodiment and multi-agent collaboration. *arXiv preprint arXiv:2505.03673*, 2025.
- [21] Enshen Zhou, Qi Su, Cheng Chi, Zhizheng Zhang, Zhongyuan Wang, Tiejun Huang, Lu Sheng, and He Wang. Code-as-monitor: Constraint-aware visual programming for reactive and proactive robotic failure detection. In *Proceedings of the Computer Vision and Pattern Recognition Conference*, pages 6919–6929, 2025.
- [22] Enshen Zhou, Jingkun An, Cheng Chi, Yi Han, Shanyu Rong, Chi Zhang, Pengwei Wang, Zhongyuan Wang, Tiejun Huang, Lu Sheng, et al. Roborefer: Towards spatial referring with reasoning in vision-language models for robotics. *arXiv preprint arXiv:2506.04308*, 2025.
- [23] Dingzhe Li, Yixiang Jin, Yuhao Sun, Hongze Yu, Jun Shi, Xiaoshuai Hao, Peng Hao, Huaping Liu, Fuchun Sun, Jianwei Zhang, et al. What foundation models can bring for robot learning in manipulation: A survey. *arXiv preprint arXiv:2404.18201*, 2024.
- [24] Zirui Song, Guangxian Ouyang, Mingzhe Li, Yuheng Ji, Chenxi Wang, Zixiang Xu, Zeyu Zhang, Xiaoqing Zhang, Qian Jiang, Zhenhao Chen, et al. Maniplvm-r1: Reinforcement learning for reasoning in embodied manipulation with large vision-language models. *arXiv preprint arXiv:2505.16517*, 2025.
- [25] Xiaoshuai Hao, Yunfeng Diao, Mengchuan Wei, Yifan Yang, Peng Hao, Rong Yin, Hui Zhang, Weiming Li, Shu Zhao, and Yu Liu. Mapfusion: A novel bev feature fusion network for multi-modal map construction. *Information Fusion*, page 103018, 2025.
- [26] Xiaoshuai Hao, Mengchuan Wei, Yifan Yang, Haimei Zhao, Hui Zhang, Yi Zhou, Qiang Wang, Weiming Li, Lingdong Kong, and Jing Zhang. Is your HD map constructor reliable under sensor corruptions? In *Advances in Neural Information Processing Systems*, 2024.
- [27] Xiaoshuai Hao, Ruikai Li, Hui Zhang, Dingzhe Li, Rong Yin, Sangil Jung, Seung-In Park, ByungIn Yoo, Haimei Zhao, and Jing Zhang. Mapdistill: Boosting efficient camera-based hd map construction via camera-lidar fusion model distillation. In *European Conference on Computer Vision*, pages 166–183, 2024.
- [28] Xiaoshuai Hao, Hui Zhang, Yifan Yang, Yi Zhou, Sangil Jung, Seung-In Park, and ByungIn Yoo. Mbfusion: A new multi-modal bev feature fusion method for hd map construction. In *IEEE International Conference on Robotics and Automation*, pages 15922–15928, 2024.
- [29] Xiaoshuai Hao, Guanqun Liu, Yuting Zhao, Yuheng Ji, Mengchuan Wei, Haimei Zhao, Lingdong Kong, Rong Yin, and Yu Liu. Msc-bench: Benchmarking and analyzing multi-sensor corruption for driving perception. *arXiv preprint arXiv:2501.01037*, 2025.
- [30] Yuting Zhao, Yuheng Ji, Xiaoshuai Hao, and Shuxiao Li. Fastrsr: Efficient and accurate road surface reconstruction from bird’s eye view. *arXiv preprint arXiv:2504.09535*, 2025.
- [31] Xiaoshuai Hao, Yuting Zhao, Yuheng Ji, Luanyuan Dai, Peng Hao, Dingzhe Li, Shuai Cheng, and Rong Yin. What really matters for robust multi-sensor hd map construction? *arXiv preprint arXiv:2507.01484*, 2025.

- [32] Artur d’Avila Garcez, Marco Gori, Luis C Lamb, Luciano Serafini, Michael Spranger, and Son N Tran. Neural-symbolic computing: An effective methodology for principled integration of machine learning and reasoning. *arXiv preprint arXiv:1905.06088*, 2019.
- [33] Saeed Amizadeh, Hamid Palangi, Alex Polozov, Yichen Huang, and Kazuhito Koishida. Neuro-symbolic visual reasoning: Disentangling. In *International Conference on Machine Learning*, pages 279–290. Pmlr, 2020.
- [34] Minkyu Choi, Harsh Goel, Mohammad Omama, Yunhao Yang, Sahil Shah, and Sandeep Chinchali. Towards neuro-symbolic video understanding. In *European Conference on Computer Vision*, pages 220–236. Springer, 2024.
- [35] Mingyu Zhang, Jiting Cai, Mingyu Liu, Yue Xu, Cewu Lu, and Yong-Lu Li. Take a step back: Rethinking the two stages in visual reasoning. In *European Conference on Computer Vision*, pages 124–141. Springer, 2024.
- [36] Tanmay Gupta and Aniruddha Kembhavi. Visual programming: Compositional visual reasoning without training. In *IEEE/CVF Conference on Computer Vision and Pattern Recognition*, pages 14953–14962, 2023.
- [37] Guowei Xu, Peng Jin, Li Hao, Yibing Song, Lichao Sun, and Li Yuan. Llava-o1: Let vision language models reason step-by-step. *arXiv preprint arXiv:2411.10440*, 2024.
- [38] Omkar Thawakar, Dinura Dissanayake, Ketan More, Ritesh Thawkar, Ahmed Heakl, Noor Ahsan, Yuhao Li, Mohammed Zumri, Jean Lahoud, Rao Muhammad Anwer, et al. Llamav-o1: Rethinking step-by-step visual reasoning in llms. *arXiv preprint arXiv:2501.06186*, 2025.
- [39] Daya Guo, Dejian Yang, Haowei Zhang, Junxiao Song, Ruoyu Zhang, Runxin Xu, Qihao Zhu, Shirong Ma, Peiyi Wang, Xiao Bi, et al. Deepseek-r1: Incentivizing reasoning capability in llms via reinforcement learning. *arXiv preprint arXiv:2501.12948*, 2025.
- [40] Kimi Team, Angang Du, Bofei Gao, Bowei Xing, Changjiu Jiang, Cheng Chen, Cheng Li, Chenjun Xiao, Chenzhuang Du, Chonghua Liao, et al. Kimi k1. 5: Scaling reinforcement learning with llms. *arXiv preprint arXiv:2501.12599*, 2025.
- [41] Pan Lu, Hritik Bansal, Tony Xia, Jiacheng Liu, Chunyuan Li, Hannaneh Hajishirzi, Hao Cheng, Kai-Wei Chang, Michel Galley, and Jianfeng Gao. Mathvista: Evaluating mathematical reasoning of foundation models in visual contexts. *arXiv preprint arXiv:2310.02255*, 2023.
- [42] Xiaoshuai Hao, Yi Zhu, Srikanth Appalaraju, Aston Zhang, Wanqian Zhang, Bo Li, and Mu Li. Mixgen: A new multi-modal data augmentation. In *IEEE/CVF winter conference on applications of computer vision*, pages 379–389, 2023.
- [43] Yue Ma, Yulong Liu, Qiyuan Zhu, Ayden Yang, Kunyu Feng, Xinhua Zhang, Zhifeng Li, Sirui Han, Chenyang Qi, and Qifeng Chen. Follow-your-motion: Video motion transfer via efficient spatial-temporal decoupled finetuning. *arXiv preprint arXiv:2506.05207*, 2025.
- [44] Yue Ma, Hongyu Liu, Hongfa Wang, Heng Pan, Yingqing He, Junkun Yuan, Ailing Zeng, Chengfei Cai, Heung-Yeung Shum, Wei Liu, et al. Follow-your-emoji: Fine-controllable and expressive freestyle portrait animation. In *SIGGRAPH Asia 2024 Conference Papers*, pages 1–12, 2024.
- [45] Yue Ma, Xiaodong Cun, Yingqing He, Chenyang Qi, Xintao Wang, Ying Shan, Xiu Li, and Qifeng Chen. Magicstick: Controllable video editing via control handle transformations. *arXiv preprint arXiv:2312.03047*, 2023.
- [46] Yue Ma, Yingqing He, Xiaodong Cun, Xintao Wang, Siran Chen, Xiu Li, and Qifeng Chen. Follow your pose: Pose-guided text-to-video generation using pose-free videos. In *Proceedings of the AAAI Conference on Artificial Intelligence*, volume 38, pages 4117–4125, 2024.
- [47] Yue Ma, Yali Wang, Yue Wu, Ziyu Lyu, Siran Chen, Xiu Li, and Yu Qiao. Visual knowledge graph for human action reasoning in videos. In *Proceedings of the 30th ACM International Conference on Multimedia*, pages 4132–4141, 2022.
- [48] Zexuan Yan, Yue Ma, Chang Zou, Wenteng Chen, Qifeng Chen, and Linfeng Zhang. Eedit: Rethinking the spatial and temporal redundancy for efficient image editing. *arXiv preprint arXiv:2503.10270*, 2025.
- [49] Kunyu Feng, Yue Ma, Xinhua Zhang, Boshi Liu, Yikuang Yuluo, Yinhan Zhang, Runtao Liu, Hongyu Liu, Zhiyuan Qin, Shanhui Mo, et al. Follow-your-instruction: A comprehensive mllm agent for world data synthesis. *arXiv preprint arXiv:2508.05580*, 2025.

[50] Yikuang Yuluo, Yue Ma, Kuan Shen, Tongtong Jin, Wang Liao, Yangpu Ma, and Fuquan Wang. Follow-your-shape: Shape-aware image editing via trajectory-guided region control. *arXiv preprint arXiv:2508.08134*, 2025.

[51] Zhuowan Li, Xingrui Wang, Elias Stengel-Eskin, Adam Kortylewski, Wufei Ma, Benjamin Van Durme, and Alan L Yuille. Super-clevr: A virtual benchmark to diagnose domain robustness in visual reasoning. In *IEEE/CVF conference on computer vision and pattern recognition*, pages 14963–14973, 2023.

[52] Jiahui Gao, Renjie Pi, Jipeng Zhang, Jiacheng Ye, Wanjun Zhong, Yufei Wang, Lanqing Hong, Jianhua Han, Hang Xu, Zhenguo Li, et al. G-llava: Solving geometric problem with multi-modal large language model. *arXiv preprint arXiv:2312.11370*, 2023.

[53] Mehran Kazemi, Hamidreza Alvari, Ankit Anand, Jialin Wu, Xi Chen, and Radu Soricut. Geomverse: A systematic evaluation of large models for geometric reasoning. *arXiv preprint arXiv:2312.12241*, 2023.

[54] Renrui Zhang, Xinyu Wei, Dongzhi Jiang, Ziyu Guo, Shicheng Li, Yichi Zhang, Chengzhuo Tong, Jiaming Liu, Aojun Zhou, Bin Wei, et al. Mavis: Mathematical visual instruction tuning with an automatic data engine. *arXiv preprint arXiv:2407.08739*, 2024.

[55] Wenhao Shi, Zhiqiang Hu, Yi Bin, Junhua Liu, Yang Yang, See-Kiong Ng, Lidong Bing, and Roy Ka-Wei Lee. Math-llava: Bootstrapping mathematical reasoning for multimodal large language models. *arXiv preprint arXiv:2406.17294*, 2024.

[56] Xin Hong, Yanyan Lan, Liang Pang, Jiafeng Guo, and Xueqi Cheng. Transformation driven visual reasoning. In *IEEE/CVF Conference on computer vision and pattern recognition*, pages 6903–6912, 2021.

[57] Yuheng Ji, Yipu Wang, Yuyang Liu, Xiaoshuai Hao, Yue Liu, Yuting Zhao, Huaihai Lyu, and Xiaolong Zheng. Visualtrans: A benchmark for real-world visual transformation reasoning. *arXiv preprint arXiv:2508.04043*, 2025.

[58] Pan Lu, Swaroop Mishra, Tanglin Xia, Liang Qiu, Kai-Wei Chang, Song-Chun Zhu, Oyvind Tafjord, Peter Clark, and Ashwin Kalyan. Learn to explain: Multimodal reasoning via thought chains for science question answering. *Advances in Neural Information Processing Systems*, pages 2507–2521, 2022.

[59] Aniruddha Kembhavi, Mike Salvato, Eric Kolve, Minjoon Seo, Hannaneh Hajishirzi, and Ali Farhadi. A diagram is worth a dozen images. In *European Conference on Computer Vision*, pages 235–251, 2016.

[60] Yingdong Hu, Fanqi Lin, Tong Zhang, Li Yi, and Yang Gao. Look before you leap: Unveiling the power of gpt-4v in robotic vision-language planning. *arXiv preprint arXiv:2311.17842*, 2023.

[61] Peng Hao, Chaofan Zhang, Dingzhe Li, Xiaoge Cao, Xiaoshuai Hao, Shaowei Cui, and Shuo Wang. Tla: Tactile-language-action model for contact-rich manipulation. *arXiv preprint arXiv:2503.08548*, 2025.

[62] Justin Johnson, Bharath Hariharan, Laurens Van Der Maaten, Judy Hoffman, Li Fei-Fei, C Lawrence Zitnick, and Ross Girshick. Inferring and executing programs for visual reasoning. In *IEEE international conference on computer vision*, pages 2989–2998, 2017.

[63] Dídac Surís, Sachit Menon, and Carl Vondrick. Vipergpt: Visual inference via python execution for reasoning. In *IEEE/CVF International Conference on Computer Vision*, pages 11888–11898, 2023.

[64] Jason Wei, Xuezhi Wang, Dale Schuurmans, Maarten Bosma, Fei Xia, Ed Chi, Quoc V Le, Denny Zhou, et al. Chain-of-thought prompting elicits reasoning in large language models. *Advances in neural information processing systems*, pages 24824–24837, 2022.

[65] Yuhao Dong, Zuyan Liu, Hai-Long Sun, Jingkang Yang, Winston Hu, Yongming Rao, and Ziwei Liu. Insight-v: Exploring long-chain visual reasoning with multimodal large language models. *arXiv preprint arXiv:2411.14432*, 2024.

[66] Daya Guo, Dejian Yang, Haowei Zhang, Junxiao Song, Ruoyu Zhang, Runxin Xu, Qihao Zhu, Shirong Ma, Peiyi Wang, Xiao Bi, et al. Deepseek-r1: Incentivizing reasoning capability in llms via reinforcement learning. *arXiv preprint arXiv:2501.12948*, 2025.

[67] Yingbo Tang, Shuaike Zhang, Xiaoshuai Hao, Pengwei Wang, Jianlong Wu, Zhongyuan Wang, and Shanghang Zhang. Affordgrasp: In-context affordance reasoning for open-vocabulary task-oriented grasping in clutter. *arXiv preprint arXiv:2503.00778*, 2025.

[68] Lingfeng Zhang, Xiaoshuai Hao, Qinwen Xu, Qiang Zhang, Xinyao Zhang, Pengwei Wang, Jing Zhang, Zhongyuan Wang, Shanghang Zhang, and Renjing Xu. Mapnav: A novel memory representation via annotated semantic maps for vlm-based vision-and-language navigation. *arXiv preprint arXiv:2502.13451*, 2025.

[69] Komal Kumar, Tajamul Ashraf, Omkar Thawakar, Rao Muhammad Anwer, Hisham Cholakkal, Mubarak Shah, Ming-Hsuan Yang, Phillip HS Torr, Salman Khan, and Fahad Shahbaz Khan. Llm post-training: A deep dive into reasoning large language models. *arXiv preprint arXiv:2502.21321*, 2025.

[70] Tianzhe Chu, Yuexiang Zhai, Jihan Yang, Shengbang Tong, Saining Xie, Dale Schuurmans, Quoc V Le, Sergey Levine, and Yi Ma. Sft memorizes, rl generalizes: A comparative study of foundation model post-training. *arXiv preprint arXiv:2501.17161*, 2025.

[71] Jason Wei, Xuezhi Wang, Dale Schuurmans, Maarten Bosma, Fei Xia, Ed Chi, Quoc V Le, Denny Zhou, et al. Chain-of-thought prompting elicits reasoning in large language models. *Advances in neural information processing systems*, pages 24824–24837, 2022.

[72] Ke Wang, Houxing Ren, Aojun Zhou, Zimu Lu, Sichun Luo, Weikang Shi, Renrui Zhang, Linqi Song, Mingjie Zhan, and Hongsheng Li. Mathcoder: Seamless code integration in llms for enhanced mathematical reasoning. *arXiv preprint arXiv:2310.03731*, 2023.

[73] Daniel M Ziegler, Nisan Stiennon, Jeffrey Wu, Tom B Brown, Alec Radford, Dario Amodei, Paul Christiano, and Geoffrey Irving. Fine-tuning language models from human preferences. *arXiv preprint arXiv:1909.08593*, 2019.

[74] Long Ouyang, Jeffrey Wu, Xu Jiang, Diogo Almeida, Carroll Wainwright, Pamela Mishkin, Chong Zhang, Sandhini Agarwal, Katarina Slama, Alex Ray, et al. Training language models to follow instructions with human feedback. *Advances in neural information processing systems*, pages 27730–27744, 2022.

[75] Zhiqing Sun, Sheng Shen, Shengcao Cao, Haotian Liu, Chunyuan Li, Yikang Shen, Chuang Gan, Liang-Yan Gui, Yu-Xiong Wang, Yiming Yang, et al. Aligning large multimodal models with factually augmented rlhf. *arXiv preprint arXiv:2309.14525*, 2023.

[76] Haipeng Luo, Qingfeng Sun, Can Xu, Pu Zhao, Jianguang Lou, Chongyang Tao, Xiubo Geng, Qingwei Lin, Shifeng Chen, and Dongmei Zhang. Wizardmath: Empowering mathematical reasoning for large language models via reinforced evol-instruct. *arXiv preprint arXiv:2308.09583*, 2023.

[77] Simon Zhai, Hao Bai, Zipeng Lin, Jiayi Pan, Peter Tong, Yifei Zhou, Alane Suhr, Saining Xie, Yann LeCun, Yi Ma, et al. Fine-tuning large vision-language models as decision-making agents via reinforcement learning. *Advances in Neural Information Processing Systems*, pages 110935–110971, 2025.

[78] Jason Wei, Maarten Bosma, Vincent Y Zhao, Kelvin Guu, Adams Wei Yu, Brian Lester, Nan Du, Andrew M Dai, and Quoc V Le. Finetuned language models are zero-shot learners. *arXiv preprint arXiv:2109.01652*, 2021.

[79] Abhimanyu Dubey, Abhinav Jauhri, Abhinav Pandey, Abhishek Kadian, Ahmad Al-Dahle, Aiesha Letman, Akhil Mathur, Alan Schelten, Amy Yang, Angela Fan, et al. The llama 3 herd of models. *arXiv preprint arXiv:2407.21783*, 2024.

[80] Bo Adler, Niket Agarwal, Ashwath Aithal, Dong H Anh, Pallab Bhattacharya, Annika Brundyn, Jared Casper, Bryan Catanzaro, Sharon Clay, Jonathan Cohen, et al. Nemotron-4 340b technical report. *arXiv preprint arXiv:2406.11704*, 2024.

[81] Rafael Rafailov, Archit Sharma, Eric Mitchell, Christopher D Manning, Stefano Ermon, and Chelsea Finn. Direct preference optimization: Your language model is secretly a reward model. *Advances in Neural Information Processing Systems*, pages 53728–53741, 2023.

[82] Nathan Lambert, Jacob Morrison, Valentina Pyatkin, Shengyi Huang, Hamish Ivison, Faeze Brahman, Lester James V Miranda, Alisa Liu, Nouha Dziri, Shane Lyu, et al. T\ ulu 3: Pushing frontiers in open language model post-training. *arXiv preprint arXiv:2411.15124*, 2024.

[83] Aixin Liu, Bei Feng, Bing Xue, Bingxuan Wang, Bochao Wu, Chengda Lu, Chenggang Zhao, Chengqi Deng, Chenyu Zhang, Chong Ruan, et al. Deepseek-v3 technical report. *arXiv preprint arXiv:2412.19437*, 2024.

[84] Zhihong Shao, Peiyi Wang, Qihao Zhu, Runxin Xu, Junxiao Song, Xiao Bi, Haowei Zhang, Mingchuan Zhang, YK Li, Y Wu, et al. Deepseekmath: Pushing the limits of mathematical reasoning in open language models. *arXiv preprint arXiv:2402.03300*, 2024.

[85] Pan Lu, Ran Gong, Shibiao Jiang, Liang Qiu, Siyuan Huang, Xiaodan Liang, and Song-Chun Zhu. Inter-gps: Interpretable geometry problem solving with formal language and symbolic reasoning. *arXiv preprint arXiv:2105.04165*, 2021.

[86] Kaichen Zhang, Bo Li, Peiyuan Zhang, Fanyi Pu, Joshua Adrian Cahyono, Kairui Hu, Shuai Liu, Yuanhan Zhang, Jingkang Yang, Chunyuan Li, et al. Lmms-eval: Reality check on the evaluation of large multimodal models. *arXiv preprint arXiv:2407.12772*, 2024.

[87] Peng Wang, Shuai Bai, Sinan Tan, Shijie Wang, Zhihao Fan, Jinze Bai, Keqin Chen, Xuejing Liu, Jialin Wang, Wenbin Ge, Yang Fan, Kai Dang, Mengfei Du, Xuancheng Ren, Rui Men, Dayiheng Liu, Chang Zhou, Jingren Zhou, and Junyang Lin. Qwen2-vl: Enhancing vision-language model's perception of the world at any resolution. *arXiv preprint arXiv:2409.12191*, 2024.

[88] Huggingface. open-r1: Fully open reproduction of deepseek-r1. <https://github.com/huggingface/open-r1>, 2025. [Online; accessed: 2025-01-24].

[89] Woosuk Kwon, Zhuohan Li, Siyuan Zhuang, Ying Sheng, Lianmin Zheng, Cody Hao Yu, Joseph E. Gonzalez, Hao Zhang, and Ion Stoica. Efficient memory management for large language model serving with pagedattention. In *ACM SIGOPS 29th Symposium on Operating Systems Principles*, 2023.

[90] Shuai Bai, Keqin Chen, Xuejing Liu, Jialin Wang, Wenbin Ge, Sibo Song, Kai Dang, Peng Wang, Shijie Wang, Jun Tang, Humen Zhong, Yuanzhi Zhu, Mingkun Yang, Zhaohai Li, Jianqiang Wan, Pengfei Wang, Wei Ding, Zheren Fu, Yiheng Xu, Jiabo Ye, Xi Zhang, Tianbao Xie, Zesen Cheng, Hang Zhang, Zhibo Yang, Haiyang Xu, and Junyang Lin. Qwen2.5-vl technical report. *arXiv preprint arXiv:2502.13923*, 2025.

[91] Marah Abdin, Jyoti Aneja, Hany Awadalla, Ahmed Awadallah, Ammar Ahmad Awan, Nguyen Bach, Amit Bahree, Arash Bakhtiari, Jianmin Bao, Harkirat Behl, et al. Phi-3 technical report: A highly capable language model locally on your phone. *arXiv preprint arXiv:2404.14219*, 2024.

[92] Zhe Chen, Jiannan Wu, Wenhui Wang, Weijie Su, Guo Chen, Sen Xing, Muyan Zhong, Qinglong Zhang, Xizhou Zhu, Lewei Lu, et al. Internvl: Scaling up vision foundation models and aligning for generic visual-linguistic tasks. In *IEEE/CVF conference on computer vision and pattern recognition*, pages 24185–24198, 2024.

[93] Meta AI. Llama 3 at connect 2024: Vision for edge and mobile devices, 2024. Accessed: 2025-02-15.

[94] Pravesh Agrawal, Szymon Antoniak, Emma Bou Hanna, Baptiste Bout, Devendra Chaplot, Jessica Chudnovsky, Diogo Costa, Baudouin De Moncault, Saurabh Garg, Theophile Gervet, et al. Pixtral 12b. *arXiv preprint arXiv:2410.07073*, 2024.

[95] Aaron Hurst, Adam Lerer, Adam P Goucher, Adam Perelman, Aditya Ramesh, Aidan Clark, AJ Ostrow, Akila Welihinda, Alan Hayes, Alec Radford, et al. Gpt-4o system card. *arXiv preprint arXiv:2410.21276*, 2024.

[96] Gemini Team, Petko Georgiev, Ving Ian Lei, Ryan Burnell, Libin Bai, Anmol Gulati, Garrett Tanzer, Damien Vincent, Zhufeng Pan, Shibo Wang, et al. Gemini 1.5: Unlocking multimodal understanding across millions of tokens of context. *arXiv preprint arXiv:2403.05530*, 2024.

[97] Xiang Yue, Yuansheng Ni, Kai Zhang, Tianyu Zheng, Ruoqi Liu, Ge Zhang, Samuel Stevens, Dongfu Jiang, Weiming Ren, Yuxuan Sun, et al. Mmmu: A massive multi-discipline multi-modal understanding and reasoning benchmark for expert agi. In *Proceedings of the IEEE/CVF Conference on Computer Vision and Pattern Recognition*, pages 9556–9567, 2024.

[98] Grok-1.5 Team. Grok-1.5 vision preview. <https://x.ai/news/grok-1.5v>, 2024. [Online; accessed: 2024-04-12].

[99] Ke Wang, Junting Pan, Weikang Shi, Zimu Lu, Houxing Ren, Aojun Zhou, Mingjie Zhan, and Hongsheng Li. Measuring multimodal mathematical reasoning with math-vision dataset. *Advances in Neural Information Processing Systems*, 37:95095–95169, 2024.

[100] Tuomo Hiippala, Malihe Alikhani, Jonas Haverinen, Timo Kalliokoski, Evanfiya Logacheva, Serafina Orekhova, Aino Tuomainen, Matthew Stone, and John A Bateman. Ai2d-rst: a multimodal corpus of 1000 primary school science diagrams. *Language Resources and Evaluation*, 55:661–688, 2021.

[101] Pan Lu, Swaroop Mishra, Tanglin Xia, Liang Qiu, Kai-Wei Chang, Song-Chun Zhu, Oyvind Tafjord, Peter Clark, and Ashwin Kalyan. Learn to explain: Multimodal reasoning via thought chains for science question answering. *Advances in Neural Information Processing Systems*, 35:2507–2521, 2022.

[102] Yanbin Wei, Shuai Fu, Weisen Jiang, Zejian Zhang, Zhixiong Zeng, Qi Wu, James Kwok, and Yu Zhang. Gita: Graph to visual and textual integration for vision-language graph reasoning. *Advances in Neural Information Processing Systems*, 37:44–72, 2024.

[103] Yew Ken Chia, Vernon Toh Yan Han, Deepanway Ghosal, Lidong Bing, and Soujanya Poria. Puzzlevqa: Diagnosing multimodal reasoning challenges of language models with abstract visual patterns. *arXiv preprint arXiv:2403.13315*, 2024.

[104] Pan Lu, Liang Qiu, Jiaqi Chen, Tony Xia, Yizhou Zhao, Wei Zhang, Zhou Yu, Xiaodan Liang, and Song-Chun Zhu. Iconqa: A new benchmark for abstract diagram understanding and visual language reasoning. *arXiv preprint arXiv:2110.13214*, 2021.

[105] Chi Zhang, Feng Gao, Baoxiong Jia, Yixin Zhu, and Song-Chun Zhu. Raven: A dataset for relational and analogical visual reasoning. In *Proceedings of the IEEE/CVF conference on computer vision and pattern recognition*, pages 5317–5327, 2019.

[106] Jiaqi Chen, Jianheng Tang, Jinghui Qin, Xiaodan Liang, Lingbo Liu, Eric P Xing, and Liang Lin. Geoqa: A geometric question answering benchmark towards multimodal numerical reasoning. *arXiv preprint arXiv:2105.14517*, 2021.

NeurIPS Paper Checklist

1. Claims

Question: Do the main claims made in the abstract and introduction accurately reflect the paper's contributions and scope?

Answer: [\[Yes\]](#)

Justification: See Section 1.

Guidelines:

- The answer NA means that the abstract and introduction do not include the claims made in the paper.
- The abstract and/or introduction should clearly state the claims made, including the contributions made in the paper and important assumptions and limitations. A No or NA answer to this question will not be perceived well by the reviewers.
- The claims made should match theoretical and experimental results, and reflect how much the results can be expected to generalize to other settings.
- It is fine to include aspirational goals as motivation as long as it is clear that these goals are not attained by the paper.

2. Limitations

Question: Does the paper discuss the limitations of the work performed by the authors?

Answer: [\[Yes\]](#)

Justification: See Appendix Section H Limitations and Societal Impact.

Guidelines:

- The answer NA means that the paper has no limitation while the answer No means that the paper has limitations, but those are not discussed in the paper.
- The authors are encouraged to create a separate "Limitations" section in their paper.
- The paper should point out any strong assumptions and how robust the results are to violations of these assumptions (e.g., independence assumptions, noiseless settings, model well-specification, asymptotic approximations only holding locally). The authors should reflect on how these assumptions might be violated in practice and what the implications would be.
- The authors should reflect on the scope of the claims made, e.g., if the approach was only tested on a few datasets or with a few runs. In general, empirical results often depend on implicit assumptions, which should be articulated.
- The authors should reflect on the factors that influence the performance of the approach. For example, a facial recognition algorithm may perform poorly when image resolution is low or images are taken in low lighting. Or a speech-to-text system might not be used reliably to provide closed captions for online lectures because it fails to handle technical jargon.
- The authors should discuss the computational efficiency of the proposed algorithms and how they scale with dataset size.
- If applicable, the authors should discuss possible limitations of their approach to address problems of privacy and fairness.
- While the authors might fear that complete honesty about limitations might be used by reviewers as grounds for rejection, a worse outcome might be that reviewers discover limitations that aren't acknowledged in the paper. The authors should use their best judgment and recognize that individual actions in favor of transparency play an important role in developing norms that preserve the integrity of the community. Reviewers will be specifically instructed to not penalize honesty concerning limitations.

3. Theory assumptions and proofs

Question: For each theoretical result, does the paper provide the full set of assumptions and a complete (and correct) proof?

Answer: [\[NA\]](#)

Justification: The paper does not include theoretical results or proofs but focuses on architectural innovation and empirical evaluation.

Guidelines:

- The answer NA means that the paper does not include theoretical results.
- All the theorems, formulas, and proofs in the paper should be numbered and cross-referenced.
- All assumptions should be clearly stated or referenced in the statement of any theorems.
- The proofs can either appear in the main paper or the supplemental material, but if they appear in the supplemental material, the authors are encouraged to provide a short proof sketch to provide intuition.
- Inversely, any informal proof provided in the core of the paper should be complemented by formal proofs provided in appendix or supplemental material.
- Theorems and Lemmas that the proof relies upon should be properly referenced.

4. Experimental result reproducibility

Question: Does the paper fully disclose all the information needed to reproduce the main experimental results of the paper to the extent that it affects the main claims and/or conclusions of the paper (regardless of whether the code and data are provided or not)?

Answer: [Yes]

Justification: See Section 4.

Guidelines:

- The answer NA means that the paper does not include experiments.
- If the paper includes experiments, a No answer to this question will not be perceived well by the reviewers: Making the paper reproducible is important, regardless of whether the code and data are provided or not.
- If the contribution is a dataset and/or model, the authors should describe the steps taken to make their results reproducible or verifiable.
- Depending on the contribution, reproducibility can be accomplished in various ways. For example, if the contribution is a novel architecture, describing the architecture fully might suffice, or if the contribution is a specific model and empirical evaluation, it may be necessary to either make it possible for others to replicate the model with the same dataset, or provide access to the model. In general, releasing code and data is often one good way to accomplish this, but reproducibility can also be provided via detailed instructions for how to replicate the results, access to a hosted model (e.g., in the case of a large language model), releasing of a model checkpoint, or other means that are appropriate to the research performed.
- While NeurIPS does not require releasing code, the conference does require all submissions to provide some reasonable avenue for reproducibility, which may depend on the nature of the contribution. For example
 - (a) If the contribution is primarily a new algorithm, the paper should make it clear how to reproduce that algorithm.
 - (b) If the contribution is primarily a new model architecture, the paper should describe the architecture clearly and fully.
 - (c) If the contribution is a new model (e.g., a large language model), then there should either be a way to access this model for reproducing the results or a way to reproduce the model (e.g., with an open-source dataset or instructions for how to construct the dataset).
 - (d) We recognize that reproducibility may be tricky in some cases, in which case authors are welcome to describe the particular way they provide for reproducibility. In the case of closed-source models, it may be that access to the model is limited in some way (e.g., to registered users), but it should be possible for other researchers to have some path to reproducing or verifying the results.

5. Open access to data and code

Question: Does the paper provide open access to the data and code, with sufficient instructions to faithfully reproduce the main experimental results, as described in supplemental material?

Answer: [\[Yes\]](#)

Justification: See supplementary material.

Guidelines:

- The answer NA means that paper does not include experiments requiring code.
- Please see the NeurIPS code and data submission guidelines (<https://nips.cc/public/guides/CodeSubmissionPolicy>) for more details.
- While we encourage the release of code and data, we understand that this might not be possible, so “No” is an acceptable answer. Papers cannot be rejected simply for not including code, unless this is central to the contribution (e.g., for a new open-source benchmark).
- The instructions should contain the exact command and environment needed to run to reproduce the results. See the NeurIPS code and data submission guidelines (<https://nips.cc/public/guides/CodeSubmissionPolicy>) for more details.
- The authors should provide instructions on data access and preparation, including how to access the raw data, preprocessed data, intermediate data, and generated data, etc.
- The authors should provide scripts to reproduce all experimental results for the new proposed method and baselines. If only a subset of experiments are reproducible, they should state which ones are omitted from the script and why.
- At submission time, to preserve anonymity, the authors should release anonymized versions (if applicable).
- Providing as much information as possible in supplemental material (appended to the paper) is recommended, but including URLs to data and code is permitted.

6. Experimental setting/details

Question: Does the paper specify all the training and test details (e.g., data splits, hyper-parameters, how they were chosen, type of optimizer, etc.) necessary to understand the results?

Answer: [\[Yes\]](#)

Justification: See Section 4 Implementation details and Appendix Sec. B.

Guidelines:

- The answer NA means that the paper does not include experiments.
- The experimental setting should be presented in the core of the paper to a level of detail that is necessary to appreciate the results and make sense of them.
- The full details can be provided either with the code, in appendix, or as supplemental material.

7. Experiment statistical significance

Question: Does the paper report error bars suitably and correctly defined or other appropriate information about the statistical significance of the experiments?

Answer: [\[Yes\]](#)

Justification: We use five various seeds to train the model and report the average accuracy of them to avoid randomness.

Guidelines:

- The answer NA means that the paper does not include experiments.
- The authors should answer “Yes” if the results are accompanied by error bars, confidence intervals, or statistical significance tests, at least for the experiments that support the main claims of the paper.
- The factors of variability that the error bars are capturing should be clearly stated (for example, train/test split, initialization, random drawing of some parameter, or overall run with given experimental conditions).
- The method for calculating the error bars should be explained (closed form formula, call to a library function, bootstrap, etc.)
- The assumptions made should be given (e.g., Normally distributed errors).

- It should be clear whether the error bar is the standard deviation or the standard error of the mean.
- It is OK to report 1-sigma error bars, but one should state it. The authors should preferably report a 2-sigma error bar than state that they have a 96% CI, if the hypothesis of Normality of errors is not verified.
- For asymmetric distributions, the authors should be careful not to show in tables or figures symmetric error bars that would yield results that are out of range (e.g. negative error rates).
- If error bars are reported in tables or plots, The authors should explain in the text how they were calculated and reference the corresponding figures or tables in the text.

8. Experiments compute resources

Question: For each experiment, does the paper provide sufficient information on the computer resources (type of compute workers, memory, time of execution) needed to reproduce the experiments?

Answer: [\[Yes\]](#)

Justification: See Section 4 Implementation details.

Guidelines:

- The answer NA means that the paper does not include experiments.
- The paper should indicate the type of compute workers CPU or GPU, internal cluster, or cloud provider, including relevant memory and storage.
- The paper should provide the amount of compute required for each of the individual experimental runs as well as estimate the total compute.
- The paper should disclose whether the full research project required more compute than the experiments reported in the paper (e.g., preliminary or failed experiments that didn't make it into the paper).

9. Code of ethics

Question: Does the research conducted in the paper conform, in every respect, with the NeurIPS Code of Ethics <https://neurips.cc/public/EthicsGuidelines>?

Answer: [\[Yes\]](#)

Justification: We have read the NeurIPS Code of Ethics, and our paper does not have these problems.

Guidelines:

- The answer NA means that the authors have not reviewed the NeurIPS Code of Ethics.
- If the authors answer No, they should explain the special circumstances that require a deviation from the Code of Ethics.
- The authors should make sure to preserve anonymity (e.g., if there is a special consideration due to laws or regulations in their jurisdiction).

10. Broader impacts

Question: Does the paper discuss both potential positive societal impacts and negative societal impacts of the work performed?

Answer: [\[Yes\]](#)

Justification: See Appendix H Limitations and Societal Impact.

Guidelines:

- The answer NA means that there is no societal impact of the work performed.
- If the authors answer NA or No, they should explain why their work has no societal impact or why the paper does not address societal impact.
- Examples of negative societal impacts include potential malicious or unintended uses (e.g., disinformation, generating fake profiles, surveillance), fairness considerations (e.g., deployment of technologies that could make decisions that unfairly impact specific groups), privacy considerations, and security considerations.

- The conference expects that many papers will be foundational research and not tied to particular applications, let alone deployments. However, if there is a direct path to any negative applications, the authors should point it out. For example, it is legitimate to point out that an improvement in the quality of generative models could be used to generate deepfakes for disinformation. On the other hand, it is not needed to point out that a generic algorithm for optimizing neural networks could enable people to train models that generate Deepfakes faster.
- The authors should consider possible harms that could arise when the technology is being used as intended and functioning correctly, harms that could arise when the technology is being used as intended but gives incorrect results, and harms following from (intentional or unintentional) misuse of the technology.
- If there are negative societal impacts, the authors could also discuss possible mitigation strategies (e.g., gated release of models, providing defenses in addition to attacks, mechanisms for monitoring misuse, mechanisms to monitor how a system learns from feedback over time, improving the efficiency and accessibility of ML).

11. Safeguards

Question: Does the paper describe safeguards that have been put in place for responsible release of data or models that have a high risk for misuse (e.g., pretrained language models, image generators, or scraped datasets)?

Answer: [NA]

Justification: The paper poses no such risks.

Guidelines:

- The answer NA means that the paper poses no such risks.
- Released models that have a high risk for misuse or dual-use should be released with necessary safeguards to allow for controlled use of the model, for example by requiring that users adhere to usage guidelines or restrictions to access the model or implementing safety filters.
- Datasets that have been scraped from the Internet could pose safety risks. The authors should describe how they avoided releasing unsafe images.
- We recognize that providing effective safeguards is challenging, and many papers do not require this, but we encourage authors to take this into account and make a best faith effort.

12. Licenses for existing assets

Question: Are the creators or original owners of assets (e.g., code, data, models), used in the paper, properly credited and are the license and terms of use explicitly mentioned and properly respected?

Answer: [Yes]

Justification: CC-BY 4.0.

Guidelines:

- The answer NA means that the paper does not use existing assets.
- The authors should cite the original paper that produced the code package or dataset.
- The authors should state which version of the asset is used and, if possible, include a URL.
- The name of the license (e.g., CC-BY 4.0) should be included for each asset.
- For scraped data from a particular source (e.g., website), the copyright and terms of service of that source should be provided.
- If assets are released, the license, copyright information, and terms of use in the package should be provided. For popular datasets, paperswithcode.com/datasets has curated licenses for some datasets. Their licensing guide can help determine the license of a dataset.
- For existing datasets that are re-packaged, both the original license and the license of the derived asset (if it has changed) should be provided.

- If this information is not available online, the authors are encouraged to reach out to the asset's creators.

13. New assets

Question: Are new assets introduced in the paper well documented and is the documentation provided alongside the assets?

Answer: [NA]

Justification: The paper does not release new assets.

Guidelines:

- The answer NA means that the paper does not release new assets.
- Researchers should communicate the details of the dataset/code/model as part of their submissions via structured templates. This includes details about training, license, limitations, etc.
- The paper should discuss whether and how consent was obtained from people whose asset is used.
- At submission time, remember to anonymize your assets (if applicable). You can either create an anonymized URL or include an anonymized zip file.

14. Crowdsourcing and research with human subjects

Question: For crowdsourcing experiments and research with human subjects, does the paper include the full text of instructions given to participants and screenshots, if applicable, as well as details about compensation (if any)?

Answer: [NA]

Justification: The paper does not involve crowdsourcing nor research with human subjects.

Guidelines:

- The answer NA means that the paper does not involve crowdsourcing nor research with human subjects.
- Including this information in the supplemental material is fine, but if the main contribution of the paper involves human subjects, then as much detail as possible should be included in the main paper.
- According to the NeurIPS Code of Ethics, workers involved in data collection, curation, or other labor should be paid at least the minimum wage in the country of the data collector.

15. Institutional review board (IRB) approvals or equivalent for research with human subjects

Question: Does the paper describe potential risks incurred by study participants, whether such risks were disclosed to the subjects, and whether Institutional Review Board (IRB) approvals (or an equivalent approval/review based on the requirements of your country or institution) were obtained?

Answer: [NA]

Justification: The paper does not involve crowdsourcing nor research with human subjects.

Guidelines:

- The answer NA means that the paper does not involve crowdsourcing nor research with human subjects.
- Depending on the country in which research is conducted, IRB approval (or equivalent) may be required for any human subjects research. If you obtained IRB approval, you should clearly state this in the paper.
- We recognize that the procedures for this may vary significantly between institutions and locations, and we expect authors to adhere to the NeurIPS Code of Ethics and the guidelines for their institution.
- For initial submissions, do not include any information that would break anonymity (if applicable), such as the institution conducting the review.

16. Declaration of LLM usage

Question: Does the paper describe the usage of LLMs if it is an important, original, or non-standard component of the core methods in this research? Note that if the LLM is used only for writing, editing, or formatting purposes and does not impact the core methodology, scientific rigorosity, or originality of the research, declaration is not required.

Answer: **[No]**

Justification: The core methodology and experiments do not involve LLMs. Any language editing assistance does not impact the scientific contributions.

Guidelines:

- The answer NA means that the core method development in this research does not involve LLMs as any important, original, or non-standard components.
- Please refer to our LLM policy (<https://neurips.cc/Conferences/2025/LLM>) for what should or should not be described.

Appendix

This supplementary material provides additional details on the proposed method and experimental results that could not be included in the main manuscript due to page limitations. Specifically, this appendix is organized as follows.

- Sec. A provides more details on the evaluation of reasoning tasks and discusses how we collected, filtered, and reconstructed a high-quality dataset.
- Sec. B outlines the models and training processes, providing more detailed experimental specifics.
- Sec. C presents comprehensive experimental results.
- Sec. D details the pipeline of CoT date generation.
- Sec. E presents detailed composition of diffenernt mixed CoT datasets.
- Sec. F shows the comparison of CoT quality before and after RL.
- Sec. G includes more visualization cases.
- Sec. H introduces the limitations of our Reason-RFT and its societal impact.

A Details of Evaluation Reasoning Tasks

A.1 Visual Counting

Task Definition Visual Counting is a multi-modal reasoning task that evaluates the integration of linguistic, visual, and mathematical capabilities by requiring models to solve arithmetic problems in dynamic visual scenes composed of 3D blocks with diverse attributes, including color, size, material, and shape. The task consists of four distinct reasoning types: **1) Subtraction**, which involves counting objects after removing a specified subset based on given attributes; **2) Addition**, where models must compute totals after inserting new objects with defined quantities and properties; **3) Adversarial**, a challenging variant designed as trick questions in which operations are performed on one set of objects while the query targets an unrelated or unaffected subset, testing the model’s robustness against deceptive scenarios; and **4) Multi-Hop**, which requires sequential reasoning through multiple addition or subtraction steps to arrive at the final count. This task challenges models to perform attribute-based reasoning in dynamic visual contexts, emphasizing cross-modal understanding and reasoning capabilities. Some examples are shown in Fig. 8.

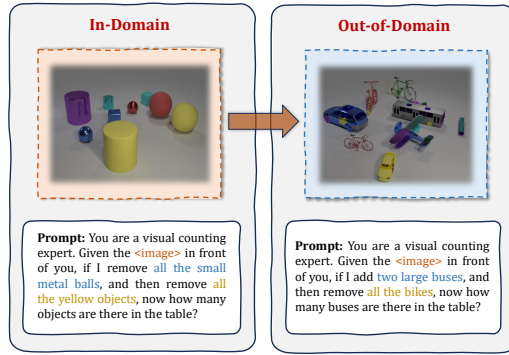


Figure 8: The sample of Visual Counting.

Dataset Preparation For In-Domain (ID) dataset, we refined the original dataset from CLEVR-Math [1] by filtering out low-quality or incorrect samples using GPT-4o, resulting in a clean dataset comprising 35K training samples and 1K test samples. These samples are categorized into four specific types: subtraction, addition, adversarial, and multihop-subtraction. To evaluate Domain-Shift (DS) generalization, we extended CLEVR-Math by enhancing the diversity of objects through the incorporation of 3D assets from Super-CLEVR [51], which leads to the creation of Super-CLEVR-Math, an advanced benchmark with 1K test samples designed to assess model generalization under increased complexity. These test samples are also divided into four task types: addition, subtraction, subtraction-multihop and addition-subtraction. The test samples are further categorized into four task types: addition, subtraction, subtraction-multihop, and addition-subtraction. The first three constitute the DS-D subset, while addition-subtraction forms the DS-M subset. Notably, the mixed addition-subtraction type introduces a novel category consisting multi-steps of both addition and subtraction, which is not present in CLEVR-Math, further elevating the benchmark’s challenge.

Reward Design Following the reward methodology of DeepSeek-R1 [39], we define two distinct reward functions: Format Reward and Accuracy Reward. The Format Reward is assigned

a value of 1 if the response adheres to the predefined template structure, specifically in the form of `<think>...</think><answer>...</answer>`; otherwise, it is assigned a value of 0. The Accuracy Reward is assigned a value of 1 if the numerical counting result in the response is correct; otherwise, it is assigned a value of 0. This dual-reward mechanism ensures both structural compliance and numerical accuracy in model responses.

A.2 Structure Perception

Task Definition Structure Perception represents a complex class of visual mathematical reasoning tasks, which focuses on assessing the model’s capacity to determine geometric structure relationships and perform calculations involving angles, lengths, areas, and other geometric properties. The task includes problems such as identifying congruent or similar shapes, calculating perimeters and areas, determining angles between lines or shapes, and solving problems related to geometric transformations (e.g., rotations, translations, and reflections). By combining mathematical rigor with visual reasoning, this task challenges models to demonstrate a deep understanding of geometric principles in both abstract and real-world scenarios. Some examples are shown in Fig. 9.

Dataset Preparation For the ID dataset, we provide GeoMath-4K5, a dataset specifically designed for geometric problem solving, which is constructed based on Math360K [55] and Geo170K [52]. To ensure data quality, we employed GPT-4o to filter out incorrect samples and removed those with answers that were neither numerical nor included in the provided options, thereby streamlining the validation process during training and testing. This refinement process resulted in a curated dataset consisting of 4.5K training samples and 820 test samples. For DS evaluation, we selected 800 samples from Geometry3K [85] (including 400 multiple-choice and 400 open-ended questions) to comprehensively assess the model’s generalization capabilities on geometry reasoning.

Reward Design We maintain the same Format Reward as used in the Visual Counting task above. The Accuracy Reward is extended to support the evaluation of both multiple-choice questions and mathematical expressions, ensuring comprehensive assessment across various problem types. Specifically, mathematical reward type is designed for Structure Perception tasks involving numerical answers, such as floating-point values or LaTeX-formatted expressions. It uses a tolerance-based evaluation to account for minor numerical deviations. The accuracy reward $R_{\text{acc}}(a_i)$ is defined as:

$$R_{\text{acc}}(a_i) = \frac{1}{2} \left[\cos \left(\pi \times \frac{|a_{\text{pred}} - a_{\text{gt}}| - \epsilon_1 \times |a_{\text{gt}}|}{(\epsilon_2 - \epsilon_1) \times |a_{\text{gt}}|} \right) + 1 \right], \quad (8)$$

where a_{pred} is the predicted answer, a_{gt} is the ground truth, ϵ_1 is the tolerance threshold for an exact match (e.g., 0.05), and ϵ_2 is the upper bound for partial rewards (e.g., 0.20). If $|a_{\text{pred}} - a_{\text{gt}}| < \epsilon_1 \times |a_{\text{gt}}|$, the reward is 1 (exact match); if $|a_{\text{pred}} - a_{\text{gt}}| > \epsilon_2 \times |a_{\text{gt}}|$, the reward is 0 (incorrect). This formulation ensures smooth transitions between full and partial rewards, enabling fair numerical evaluation.

A.3 Spatial Transformation

Task Definition Spatial Transformation is a spatial-visual reasoning task designed to infer single-step or multi-step transformation actions by analyzing the initial and final visual states from multiple perspectives (e.g., center, left, right). The task utilizes transformation functions, including `change_size`, `change_color`, `change_material`, `change_shape`, and `change_position`, to modify object properties such as size, color, material, shape, and position using predefined values. This task evaluates the model’s ability to reason about spatial relationships and object transformations across diverse viewpoints in dynamic visual scenarios. Some examples are shown in Fig. 10.

Dataset Preparation We generated 100K samples using the environment and configuration from Trance [56], with each sample comprising initial object attributes, front-view image of initial state,

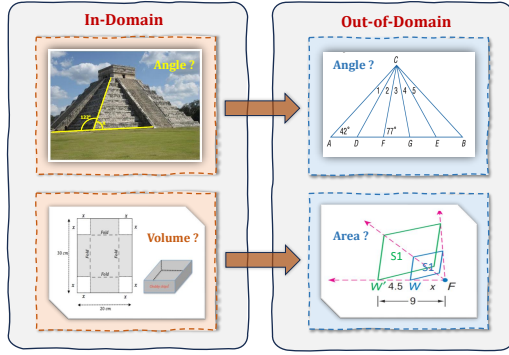


Figure 9: The sample of Structure Perception.

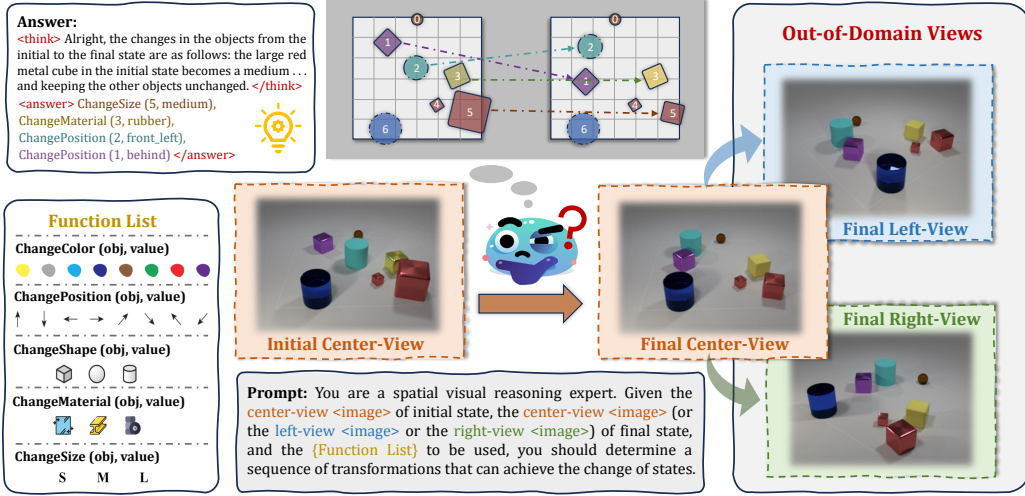


Figure 10: The sample of Spatial Transformation.

and images of final state captured from front, left, and right perspectives. To ensure high data quality, we implemented a rigorous filtering process: (1) removing samples containing occluded or invisible objects in either the initial or final states, (2) eliminating redundant actions within the transformation sequences, and (3) consolidating multi-step displacement actions, which collectively ensure the uniqueness and correctness of the solutions. The refined dataset consists of 60K training samples and 6K test samples. For the training set, we constructed the Trans-Center-60K dataset using the Center-Center configuration, which pairs front-view initial and final state images. For ID evaluation, we derived the Trans-Center-6K dataset from the 6K test samples under the same Center-Center configuration. To evaluate DS generalization, we constructed two additional datasets: Trans-Left-6K (DS-L) and Trans-Right-6K (DS-R), leveraging the Center-Left and Center-Right configurations to assess the model’s generalization capabilities in spatial reasoning under viewpoint conditions.

Reward Design For the Format Reward, we adopted the same formulation as used in the Visual Counting task. As for the Accuracy Reward, a specialized design was developed to evaluate the sequence of transformation functions. Function-based type is designed for Spatial Transformation tasks requiring a sequence of transformation functions. The accuracy reward $R_{\text{acc}}(a_i)$ evaluates the alignment between the predicted sequence T_{pred} and the ground truth T_{gt} , computed as:

$$R_{\text{acc}}(a_i) = \frac{\text{len}(T_{\text{pred}}^{f+o+v}) + \alpha \cdot \text{len}(T_{\text{pred}}^{f+o/v}) + \beta \cdot \text{len}(T_{\text{pred}}^f)}{\max(\text{len}(T_{\text{pred}}), \text{len}(T_{\text{gt}}))}, \quad (9)$$

where T_{pred}^{f+o+v} is the subset of transformation steps with complete matches (w/ function, object, and value), $T_{\text{pred}}^{f+o/v}$ are the subsets with partial and only-function matches (w/ function and object, or w/ function and value), T_{pred}^f is the subset with only-function matches. α and β are the weighting coefficients for partial matches. This formulation ensures nuanced evaluation, rewarding both exact and partially correct responses while allowing flexible adjustment of partial match contributions.

System Prompts For the Spatial Transformation task, we designed two versions of the system prompt. The first version specifies the answer output format using the `<think>` and `<answer>` tags, while the second version includes additional outputs `<summary>` and `<caption>` for experiments on exploration of format reward design in the main paper. These two versions are illustrated in Fig. 11 and Fig. 12, respectively.

B Details of Models and Training

We utilize Qwen2-VL-2B and Qwen2-VL-7B [87] as the backbone models for our experiments. Our implementation is built on the open-source frameworks Open-R1 [88] and vLLM [89], ensuring reproducibility and scalability. All experiments were conducted on a cluster of servers, each equipped with $8 \times$ A800 GPUs. For the Visual Counting task and Spatial Transformation task, we trained

Table 4: **Detailed configuration for each training stage of Reason-RFT.** The table presents the training parameters for the 2B model and 7B model across three visual reasoning tasks. The parameters marked with * correspond to Visual Counting / Structure Perception / Spatial Transformation.

		Qwen2-VL-2B		Qwen2-VL-7B	
		Stage-1	Stage-2	Stage-1	Stage-2
<i>Data</i>	Dataset	CoT dataset	Non-CoT dataset	CoT dataset	Non-CoT dataset
	#Samples	1.6K	35K / 4.5K / 60K *	1.6K	35K / 4.5K / 60K *
<i>Model</i>	Trainable Part	Full Model	Full Model	Full Model	Full Model
	#Tunable Parameters	2.21B	2.21B	8.29B	8.29B
<i>Training</i>	Per-device Batch Size	8	1	8	1
	Gradient Accumulation	2	2	2	2
	LR: $\{\psi_v^{\text{VIT}}, \phi_v^{\text{LLM}}\}$	1×10^{-5}	1×10^{-6}	1×10^{-5}	1×10^{-6}
	Epoch	1	$1/5/1^*$	1	$1/5/1^*$
	Optimizer	AdamW	AdamW	AdamW	AdamW
	Deepspeed	Zero3	Zero3	Zero3	Zero3
	Weight Decay	0.1	0.0	0.1	0.0
	Warmup Ratio	0.03	0.00	0.03	0.00
	LR Schedule	Cosine	Cosine	Cosine	Cosine
	Max Seq. Length	32768	4096	32768	4096
	Max Compl. Length	–	512	–	512
	Num. of Compl.	–	8	–	4
	GPU Nums	1×8	1×8	1×8	1×8

the models for 1 epoch each on their respective training datasets, ensuring sufficient exposure to task-specific patterns while avoiding overfitting. For the Structure Perception task, due to its GeoMath training dataset consisting of a relatively small number of training samples (a total of 4,500), we extended the training duration to 5 epochs to allow the models to fully capture the underlying structural and geometric relationships. In the Reason-RFT training pipeline, all models underwent an initial CoT activation stage with 1,600 samples before proceeding to the RL phase. More details on training process of each models are shown in Tab. 4

C More Experiment Results

Exploration on COT Activation Data To investigate the impact of differently composed CoT activation data on Reason-RFT, we construct two distinct datasets: a mixed domain-specific dataset, which integrates relevant yet distinct data from in-domain tasks, and a mixed general-domain dataset, encompassing a broader range of visual reasoning tasks (*e.g.*, graph topology, visual puzzles). The detailed dataset composition is provided in Appendix Sec. E. Using these datasets, we perform Reason-RFT training on Structure Perception task, with the results detailed in Tab. 5. From this, two key points emerge: (1) As the proportion of in-domain training data decreases, the model’s performance on specific tasks declines; (2) Models trained on more diverse visual reasoning domain data may also exhibit a reduction in domain-specific performance.

Results on Different Backbones We further validate the effectiveness of *Reason-RFT* on stronger or alternative vision–language backbones. We report results on three visual reasoning tasks: Visual Counting (T1), Structure Perception (T2), and Spatial Transformation (T3) in the combined Tab. 6. *Reason-RFT* achieves the strongest averages across backbones and tasks, with especially large margins on domain-shifted splits while keeping in-domain (ID) performance near ceiling. On **Qwen2.5-VL-3B**, for **T1** (Visual Counting) ID is already saturated (99.0 with Reason-RFT-Zero vs. 98.8 with Reason-RFT), yet *Reason-RFT* markedly improves robustness on DS: +9.2 on DS-D (68.7 vs. 59.5 vs. CoT-SFT) and +5.6 on DS-M (54.8 vs. 49.2 vs. CoT-SFT), with an especially large +44.0 over Reason-RFT-Zero on DS-M (54.8 vs. 10.8), yielding the best T1 AVG (74.1); for **T2** (Structure Perception) it is best on both ID/DS (59.0/56.6), beating CoT-SFT by +2.9 (ID) and +7.2 (DS) and Reason-RFT-Zero by +4.2 (ID) and +2.1 (DS), indicating that RL enhances stepwise structural reasoning rather than overfitting; for **T3** (Spatial Transformation) ANS-SFT

Table 5: Results of various mixed CoT activation datasets on the Structure Perception task.

Setting	CoT Activation Data	ID	DS	AVG
Baseline	GeoMath-only data	59.27	49.25	54.26
(a)	Mixed Specific-Domain data	50.61	45.35	48.02
(b)	Mixed General-Domain data	42.51	40.25	41.38

Table 6: **Results on different backbones across three tasks.** Best is **bold**; second-best is underlined. “ID” denotes in-domain; “DS- $*$ ” denotes domain-shifted splits. Missing results are shown as “–”.

Backbone	Method	Visual Counting (T1)				Structure Perception (T2)			Spatial Transformation (T3)			
		ID	DS-D	DS-M	AVG	ID	DS	AVG	ID	DS-L	DS-R	AVG
Qwen2.5-VL-3B	Zero-Shot	75.9	50.9	4.4	43.7	36.8	37.4	37.1	8.6	8.3	8.3	8.4
	+ ANS-SFT	97.4	51.5	6.0	51.6	53.0	31.8	42.4	91.1	47.0	46.8	<u>61.6</u>
	+ CoT-SFT	89.2	<u>59.5</u>	<u>49.2</u>	66.0	<u>56.1</u>	49.4	52.7	81.6	46.1	44.2	57.3
	+ Reason-RFT-Zero	99.0	58.9	10.8	56.2	54.8	<u>54.5</u>	<u>54.6</u>	68.5	<u>49.5</u>	<u>48.0</u>	55.3
	+ Reason-RFT	98.8	68.7	54.8	74.1	59.0	56.6	57.8	86.7	55.2	54.4	65.4
InternVL3-2B	Zero-Shot	79.30	51.20	5.10	45.20	–	–	–	–	–	–	–
	+ ANS-SFT	96.80	52.00	6.50	51.77	–	–	–	–	–	–	–
	+ CoT-SFT	88.90	<u>60.10</u>	<u>50.20</u>	<u>66.40</u>	–	–	–	–	–	–	–
	+ Reason-RFT-Zero	98.90	59.40	12.30	56.87	–	–	–	–	–	–	–
	+ Reason-RFT	99.10	69.80	55.90	74.93	–	–	–	–	–	–	–

attains the top ID (91.1) but is less robust, whereas *Reason-RFT* trades a modest -4.4 on ID (86.7) for substantial DS gains of $+8.2$ on DS-L (55.2 vs. 47.0) and $+7.6$ on DS-R (54.4 vs. 46.8), delivering the best AVG (65.4) and a superior ID/DS Pareto. On *InternVL3-2B* for **T1**, *Reason-RFT* is best on ID/DS-D/DS-M (99.10/69.80/55.90) and AVG (74.93), improving over ANS-SFT, CoT-SFT, and Reason-RFT-Zero by $+23.16$, $+8.53$, and $+18.06$, respectively, with the largest domain-shift margin on DS-M of $+43.60$ over Reason-RFT-Zero (55.90 vs. 12.30). Taken together, these trends across architecturally distinct backbones indicate that the benefits of *Reason-RFT* are backbone-agnostic, improving both coherence-driven reasoning and out-of-distribution reliability.

Evaluation on General Benchmarks Although *Reason-RFT* is primarily designed to enhance domain-specific visual reasoning abilities, we conduct a thorough evaluation on general benchmarks to verify whether our approach compromises the model’s general reasoning capabilities. Tab. 7 presents the results on four widely adopted datasets: MMMU [97], RealWorldQA [98], MathVision [99], and AI2D [100]. Across all tasks and model scales, *Reason-RFT* consistently maintains or even improves general performance. For instance, on the 2B model, *Reason-RFT* achieves the highest scores on MMMU

(41.14) and AI2D (75.24), outperforming both zero-shot baselines and other supervised fine-tuning approaches such as ANS-SFT and CoT-SFT. Notably, it also improves performance on the challenging MathVision task (14.82), demonstrating its robustness in spatial reasoning. For the larger 7B model, *Reason-RFT* again surpasses ANS-SFT and CoT-SFT by large margins, particularly on RealWorldQA (61.31) and MMMU (50.04), while maintaining strong results on AI2D (81.70). These results suggest that *Reason-RFT* not only scales effectively with model size but also introduces no observable performance degradation on general benchmarks. In summary, the empirical evidence supports that *Reason-RFT* enhances domain-specific reasoning while preserving—if not enhancing—general visual-language reasoning capabilities. This confirms the robustness and transferability of our method, making it a strong alternative to conventional fine-tuning paradigms.

Performance at Different Training Steps Fig. 13 and Fig. 14 illustrate the ID and DS performance of all the training methods across three visual reasoning tasks, evaluated at various training sample sizes. This analysis helps us understand how each method scales with training data. More detail evaluation results for each subset of three tasks are in Tab. 10 - Tab. 17. We systematically varied the number of training samples, from minimal to substantial, allowing us to identify performance thresholds and data efficiency for each method in both ID and DS contexts. Key findings from this analysis include: Data Efficiency of Reason-RFT: *Reason-RFT* demonstrates exceptional data efficiency, achieving approximately 70% of the performance of *Reason-RFT-Zero* with only 3% of the training data (1,600 samples), and 82.5% with just 9%. Robust Generalization to DS scenarios: In the 7B model, *Reason-RFT* achieves over 92% of *Reason-RFT-Zero*’s performance using just 3% of the training data, showcasing its strong generalization capabilities. Comparison Across Methods: *Reason-RFT* consistently outperforms other methods, particularly in data-constrained scenarios,

Table 7: Evaluation results on general benchmarks.

Method	General			
	MMMU	RealWorldQA	MathVision	AI2D
Qwen2VL-2B-Instruct				
Zero-Shot	39.89	61.31	12.50	72.50
+ ANS-SFT	<u>40.56</u>	48.76	15.79	68.20
+ CoT-SFT	34.00	37.78	12.99	65.36
+ Reason-RFT-Zero	39.30	42.81	13.00	74.61
+ Reason-RFT	41.14	<u>53.06</u>	14.82	75.24
Qwen2VL-7B-Instruct				
Zero-Shot	54.10	67.19	<u>16.30</u>	83.00
+ ANS-SFT	42.66	48.10	9.12	78.30
+ CoT-SFT	44.67	36.46	15.30	73.25
+ Reason-RFT-Zero	46.44	45.10	10.86	75.28
+ Reason-RFT	50.04	61.31	17.60	81.70

indicating its suitability for applications with limited data availability. Performance Saturation: As training sample size increases, some methods experience performance plateaus, suggesting that beyond a certain point, additional data yields diminishing returns.

In conclusion, the evaluation of performance across different training samples not only highlights the strengths of *Reason-RFT* in terms of data efficiency and generalization but also provides critical insights into the performance dynamics of various methods. These findings are essential for practitioners aiming to maximize performance while effectively managing training resources.

D More Details on CoT Data Construction

This section expands the pipeline of CoT generation by detailing both the automated and manual components used to construct our *CoT-SFT* corpus.

(1) Automated Generation. We instantiate CoT drafts using reasoning-guided prompt templates such as “*Let’s break down the problem step by step...*” and “*To answer this, we need to consider...*”. Templates are combined with model prompting (GPT-4o [95] and Gemini-Pro [96]) under temperature-controlled sampling ($T=0.7$, $\text{top-}k=50$, $\text{top-}p=0.9$). To increase coverage and depth, we insert hand-crafted, subtask-specific few-shot exemplars that bias toward explicit intermediate justifications and error-checking behavior.

(2) Automated Filtering. Each generated CoT is screened by two criteria:

Length range. For each subtask s , we compute a target trajectory length \bar{L}_s from a balanced mixture of 50% human-written and 50% model-generated samples:

$$\bar{L}_s = \frac{1}{2}(\bar{L}_s^{\text{human}} + \bar{L}_s^{\text{model}}),$$

where \bar{L}_s^{human} and \bar{L}_s^{model} are computed as sample means over their respective sets after basic deduplication. A candidate with length L_i is retained iff

$$0.6 \bar{L}_s \leq L_i \leq 1.4 \bar{L}_s,$$

where L_i is measured in tokens by our training-time tokenizer; the factors 0.6 and 1.4 were selected via a small pilot study to trim outliers while preserving diversity.

Inconsistency. We discard the responses that contradict the known ground truth, including self-inconsistent counts, incompatible algebraic steps, or reasoning that invalidates later conclusions.

For reference, the empirical trajectory-length statistics (mean μ , stdev σ) across tasks are:

Task	μ (tokens)	σ (tokens)
Visual Counting	70	30
Structural Perception	180	80
Spatial Transformation	400	120

where μ and σ are computed over the curated pool *after* automated filtering and *before* manual review.

(3) Human Verification. We randomly sample 10% of CoT drafts from each task for manual review, focusing on (i) step-to-step coherence, (ii) logical validity, and (iii) alignment between the reasoning chain and the final answer. Typical failure modes include: (i) a correct final answer supported by an incorrect chain (e.g., deriving triangle area via the Pythagorean theorem); (ii) internal contradictions, such as stating “There are 3 red blocks on the left and 2 on the right” and later concluding the total is 6. A follow-up quality audit found that, prior to human verification, approximately 3.8% of samples contained critical logical flaws; after verification, the residual error rate fell below 1%, indicating high post-cleanup reliability.

Discussion. Automated generation with calibrated sampling and subtask-specific few-shots provides diverse yet structured CoTs; the length- and consistency-based filters remove overly terse/verbose or self-contradictory drafts; targeted human verification further suppresses high-severity errors. Together, these stages yield a CoT-SFT dataset with improved coherence and faithfulness, while maintaining scalability and reproducibility.

E Detail on Mixed CoT Datasets

As shown in Tab. 8, we presents a comprehensive overview of the datasets utilized for all of our visual reasoning experiments, categorized into three experimental groups. All of them are CoT-annotated by GPT-4o [95] The Main Experiment section includes three large-scale datasets: Visual-Counting (35,000 samples) for quantitative analysis, Structure-Perception (4,500 samples) for structural understanding, and Spatial-Transformation (60,000 samples) assessing spatial reasoning capabilities. For Ablation Studies, two mixed-domain subsets were constructed: (1) The Mixed General-Domain set comprises 11 CoT-annotated datasets spanning scientific reasoning (AI2D [59], ScienceQA [101]), topological graph problems (GVLQA series [102]), and pattern recognition (PuzzleVQA [103], IconQA [104], Raven [105]). (2) The Mixed Specific-Domain set focuses exclusively on geometric reasoning, featuring GeoQA [106], GeomVerse [53], and Geometry3K [85] with progressively complex problem structures. All datasets were standardized to ensure training compatibility.

Table 8: Datasets Overview for Visual Reasoning Tasks

Dataset Name	Samples	Reasoning Type	Description
Main Experiment			
Visual-Counting	35,000	Visual Counting	Full dataset for visual counting task
Structure-Perception	4,500	Structure Perception	Full dataset for structural perception tasks
Spatial-Transformation	60,000	Spatial Transformation	Full dataset for spatial transformation tasks
Ablation Experiment (Mixed General-Domain)			
AI2D [59]	1,467	Scientific Reasoning	Scientific diagram interpretation
ScienceQA [101]	2,112	Scientific Reasoning	Science question answering
GVLQA-connectivity [102]	1,199	Topological Reasoning	Graph connectivity problems
GVLQA-cycle [102]	1,194	Topological Reasoning	Cycle detection in graphs
GVLQA-hamilton [102]	1,158	Topological Reasoning	Hamiltonian path problems
GVLQA-topology [102]	1,070	Topological Reasoning	General topology questions
GVLQA-matching [102]	1,193	Topological Reasoning	Graph matching tasks
PuzzleVQA [103]	1,618	Pattern/Puzzle	Visual puzzle solving
IconQA [104]	5,270	Pattern/Puzzle	Icon-based question answering
Raven [105]	982	Pattern/Puzzle	Raven’s Progressive Matrices
Ablation Experiment (Mixed Specific-Domain)			
GeoQA [106]	1,500	Geometric Reasoning	Geometric problem solving
GeomVerse [53]	2,841	Geometric Reasoning	Advanced geometry challenges
Geometry3K [85]	3,794	Geometric Reasoning	Comprehensive geometry problems

F Comparison of CoT Quality Before and After RL

Setting. We compare the **Qwen2VL-3B** model trained with *Reason-RFT* (Stage 2, post-RL) against the same backbone trained with only *CoT-SFT* (Stage 1, pre-RL) on the Structure Perception task. Unless otherwise noted, statistics are computed over a random sample of $n = 100$ problem instances.

Qualitative findings. Despite the high textual similarity between the two variants, the post-RL model exhibits stronger logical coherence across intermediate steps, with fewer broken or skipped chains of inference. For example, in Fig. 16 (case 2), the pre-RL model correctly infers a formula but omits the subsequent multiplication by 2, an error that is notably less frequent after RL. In addition, the post-RL model more often displays reflective behaviors (*e.g.*, “*let me double check*”) that are rarely observed in pre-RL outputs as shown in the math example of Fig. 1.

Quantitative protocol. We assess three dimensions of chain-of-thought (CoT) quality: (i) **Reasoning Step Count**—the number of explicitly delimited reasoning steps per sample, obtained via automatic counting with GPT-4o [95]; (ii) **Lexical Usage** of two categories of expressions: *Prompting words*

Table 9: Summary of comparative metrics on *Structure Perception* ($n = 100$). Positive values indicate post-RL improvements.

Metric	Change (Post-Pre)
Reasoning Step Count	+2.7 steps
Prompting Words	+14%
Logical Connectives	+23%
Answer Accuracy	+20.56%

(e.g., “*oh I see*”, “*let me think step by step*”, “*let me double check*”) and *Logical connectives* (e.g., “*so*”, “*therefore*”, “*first*”, “*but*”, “*moreover*”); and (iii) **Answer Accuracy** as reported for the accuracy rate of Structure Perception task.

Results and interpretation. Post-RL training increases the average CoT *granularity* (as reflected by the larger step count), the *organizational scaffolding* of reasoning (higher usage of prompting phrases and discourse connectives), and the *task effectiveness* (higher final-answer accuracy). Taken together, these observations indicate that reinforcement learning with Reason-RFT enhances both the coherence and utility of CoT: it reduces fragile or truncated chains, encourages reflective self-checks, and translates these behaviors into substantial accuracy gains.

G Visualization

In this section, we present additional visualization results on general visual reasoning and three specific task reasoning, see Fig. 15 - Fig. 23. Reason-RFT demonstrates superior performance over CoT-SFT in terms of logical consistency, reasoning quality, and correctness. CoT-SFT’s flaws stem from incorrect assumptions and misinterpretations, highlighting the importance of accurate problem interpretation and reasoning in visual reasoning tasks.

H Limitations and Societal Impact

Limitations While Reason-RFT has demonstrated strong performance in visual reasoning tasks, there are still areas to address. Future work will explore its application across a range of computer vision models, scaling to larger architectures (e.g., 32B/72B), and integrating large-scale Mixture of Experts (MoE) models to evaluate generalization. We will also extend the framework to complex downstream scenarios, such as embodied AI and autonomous driving, testing its effectiveness in real-world applications that require sophisticated visual reasoning and real-time decision-making.

Societal Impact The advancements of Reason-RFT in visual reasoning have important societal implications. By enhancing generalization and cross-domain transferability, this framework can improve AI applications in areas like medical imaging, autonomous driving, and assistive technologies for the visually impaired. It also reduces overfitting and cognitive rigidity, leading to more reliable and interpretable AI systems that foster trust in human-AI collaboration. The reconstructed benchmark dataset allows for fair evaluation, promoting research in robust AI. However, ethical considerations, such as biases in training data and responsible deployment, must be addressed to prevent misuse. Overall, Reason-RFT paves the way for adaptable and trustworthy AI, benefiting industries, researchers, and society.

System Prompt for Spatial Transformation Task

"Your need to complete the spatial visual reasoning task according to the following rules.

Task Description:

Given the image of the initial state, the image of the final state, and the attributes of the initial objects, you should determine a transformation that can achieve the change of states.

The **attributes** of the initial objects are provided as a list of tuples in the following format:

`*(object_id, 'shape', 'size', 'color', 'material')*`

Each tuple represents an object and its properties in the initial state.

The transformation should be a sequence of functions with a length ranging from 1 to 4, where each function is represented as `func(object_id, value)*`.

Available functions and values:

1. `change_size(object_id, value)*` - Changes the object to a new size relative to its initial size.

- Possible values: `['small', 'medium', 'large']`

2. `change_color(object_id, value)*` - Changes the object to a new color relative to its initial color.

- Possible values: `['yellow', 'gray', 'cyan', 'blue', 'brown', 'green', 'red', 'purple']`

3. `change_material(object_id, value)*` - Changes the object to a new material relative to its initial material.

- Possible values: `['glass', 'metal', 'rubber']`

4. `change_shape(object_id, value)*` - Changes the object to a new shape relative to its initial shape.

- Possible values: `['cube', 'sphere', 'cylinder']`

5. `change_position(object_id, value)*` - Moves the object to a new position relative to its initial location.

- Possible values: `['front', 'behind', 'left', 'right', 'front_left', 'front_right', 'behind_left', 'behind_right']`

- 'front' means moving forward along the object's initial direction.

- 'behind' means moving backward along the object's initial direction.

- 'left' means moving to the left of the object's initial orientation.

- 'right' means moving to the right of the object's initial orientation.

- 'front_left' means moving diagonally toward the front and left of the initial location.

- 'front_right' means moving diagonally toward the front and right of the initial location.

- 'behind_left' means moving diagonally toward the behind and left of the initial location.

- 'behind_right' means moving diagonally toward the behind and right of the initial location.

Output Format

You should first thinks about the reasoning process internally and then provides the user with the answer. The **reasoning process** and **answer** are enclosed within specific tags:

- **Reasoning process**: Provide a chain-of-thought, logical explanation of the problem. This should outline step-by-step reasoning, enclosed within `<think>...</think>`

- **Final answer (sequence of functions only)**: Enclosed within `<answer>...</answer>`

Now, it's your turn!

{Question} Output the thinking process in `<think> </think>` and final answer in `<answer> </answer>` tags.

..

Figure 11: The system prompt used in Spatial Transformation task.

System Prompt for Spatial Transformation Task (Add <summary> <caption> in FORMAT)

""Your need to complete the spatial visual reasoning task according to the following rules.

Task Description:

Given the image of the initial state, the image of the final state, and the attributes of the initial objects, you should determine a transformation that can achieve the change of states.

The **attributes of the initial objects** are provided as a list of tuples in the following format:

('object_id', 'shape', 'size', 'color', 'material')

Each tuple represents an object and its properties in the initial state.

The transformation should be a sequence of functions with a length ranging from 1 to 4, where each function is represented as **'func(object_id, value)'**.

Available functions and values:

1. **'change_size(object_id, value)'** - Changes the object to a new size relative to its initial size.

- Possible values: ['small', 'medium', 'large']

2. **'change_color(object_id, value)'** - Changes the object to a new color relative to its initial color.

- Possible values: ['yellow', 'gray', 'cyan', 'blue', 'brown', 'green', 'red', 'purple']

3. **'change_material(object_id, value)'** - Changes the object to a new material relative to its initial material.

- Possible values: ['glass', 'metal', 'rubber']

4. **'change_shape(object_id, value)'** - - Changes the object to a new shape relative to its initial shape.

- Possible values: ['cube', 'sphere', 'cylinder']

5. **'change_position(object_id, value)'** - Moves the object to a new position relative to its initial location.

- Possible values: ['front', 'behind', 'left', 'right', 'front_left', 'front_right', 'behind_left', 'behind_right']

- 'front' means moving forward along the object's initial direction.

- 'behind' means moving backward along the object's initial direction.

- 'left' means moving to the left of the object's initial orientation.

- 'right' means moving to the right of the object's initial orientation.

- 'front_left' means moving diagonally toward the front and left of the initial location.

- 'front_right' means moving diagonally toward the front and right of the initial location.

- 'behind_left' means moving diagonally toward the behind and left of the initial location.

- 'behind_right' means moving diagonally toward the behind and right of the initial location.

Output Format

You should first think about the reasoning process internally and then provide the user with the answer. The **reasoning process** and **answer** are enclosed within specific tags:

- **Summary process**: Summary how you will approach the problem and explain the steps you will take to reach the answer, enclosed within `<summary>...</summary>`

- **Caption process**: Provide a detailed description of the image, particularly emphasizing the aspects related to the question, enclosed within `<caption>...</caption>`

- **Reasoning process**: Provide a chain-of-thought, logical explanation of the problem. This should outline step-by-step reasoning, enclosed within `<think>...</think>`

- **Final answer (sequence of functions only)**: Enclosed within `<answer>...</answer>`

Now, it's your turn!

[Question] Output the summary process in <summary> </summary>, caption process in <caption>...</caption>, thinking process in <think> </think> and final answer in <answer> </answer> tags.

""

Figure 12: The system prompt used in Spatial Transformation task w/ <summary> and <caption> tags in format.

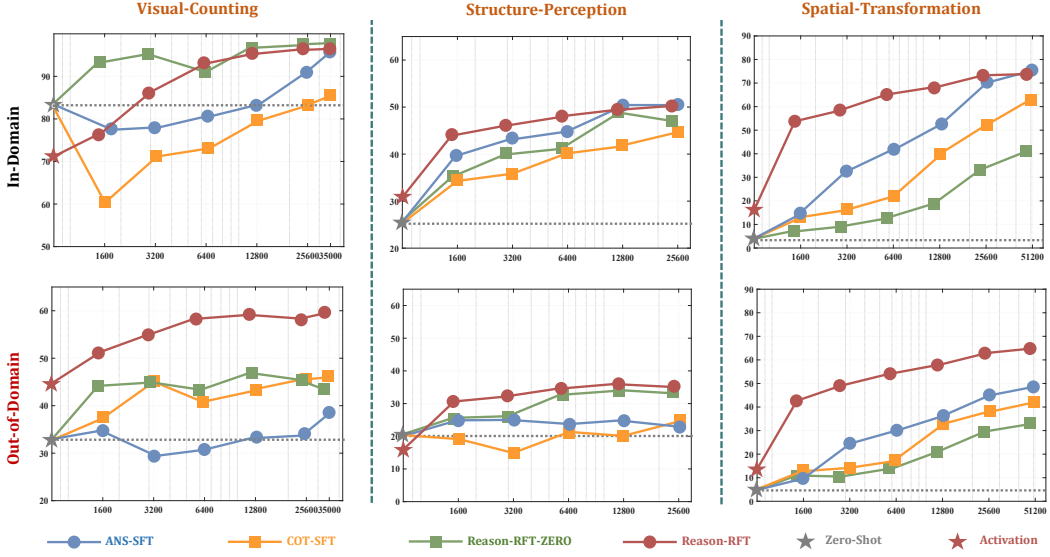


Figure 13: Results of all methods on Qwen2VL-2B-Instruct, ID and DS performance at different training checkpoints.

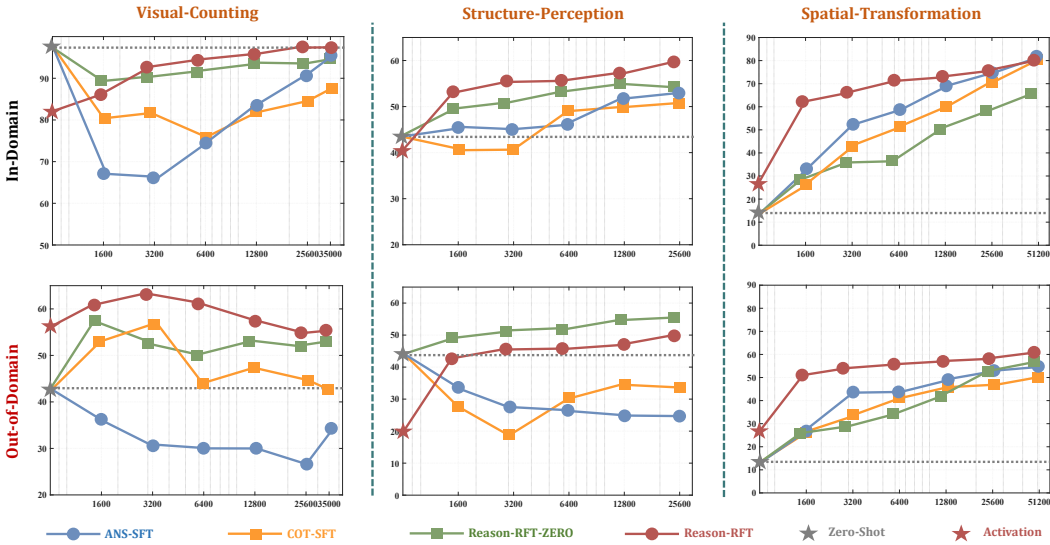


Figure 14: Results of all methods on Qwen2VL-7B-Instruct, ID and DS performance at different training checkpoints.

Methods	Steps	Visual Counting				
		Clevr-Math (ID)				
		adversarial	sub-multi	addition	subtraction	AVG
Zero-Shot	-	93.60	84.00	55.60	96.40	82.40
ANS-SFT	100	83.60	56.40	91.20	81.60	78.20
	200	69.20	67.60	91.60	82.00	77.60
	400	81.60	65.60	90.80	84.80	80.70
	600	72.40	73.20	92.40	89.20	81.80
	800	78.40	77.20	82.80	90.40	82.20
	1200	85.60	78.00	91.60	95.60	87.70
	1600	92.80	82.40	94.80	96.80	91.70
	2187	95.20	92.80	97.60	99.20	96.20
	100	49.20	40.00	82.00	69.20	60.10
CoT-SFT	200	65.20	55.60	88.00	76.40	71.30
	400	66.00	57.20	90.00	79.60	73.20
	600	67.20	59.20	87.20	82.80	74.10
	800	77.60	61.60	92.40	85.20	79.20
	1200	76.80	70.00	91.20	93.60	82.90
	1600	80.80	66.80	91.60	92.00	82.80
	2187	83.20	71.20	93.20	94.40	85.50
	100	92.80	88.80	94.40	96.00	93.00
	200	95.60	91.60	95.60	97.60	95.10
Reason-RFT-Zero	400	92.00	87.60	84.00	96.40	90.00
	600	94.40	92.80	93.60	96.00	94.20
	800	96.40	96.40	96.00	98.80	96.90
	1200	98.40	95.60	100.00	99.60	98.40
	1600	96.40	94.80	98.80	99.60	97.40
	2500	98.40	95.60	99.60	100.00	98.40
	100	89.60	73.20	93.60	95.60	88.00
	200	89.20	78.00	95.20	96.40	89.70
	400	92.80	82.40	95.20	97.60	92.00
Reason-RFT	600	94.80	86.00	96.80	97.20	93.70
	800	96.80	88.40	96.80	98.80	95.20
	1200	94.80	86.00	96.40	98.80	94.00
	1600	94.40	91.60	97.20	99.60	95.70
	2500	98.40	92.80	96.80	99.20	96.80

Table 10: Complete experimental results of Qwen2VL-2B-Instruct on the Clevr-Math test set after training on Clevr-Math. “sub-multi” donates the subtraction-multihop task.

Methods	Steps	Visual Counting						
		Super-Clevr-Math (DS)						
		addition	subtraction	add-sub	sub-multi	AVG	DS-D	DS-M
Zero-Shot	-	10.40	54.40	0.00	63.20	32.00	42.67	0.00
ANS-SFT	100	51.20	37.60	11.60	39.20	34.90	42.67	11.60
	200	38.40	55.60	8.40	15.60	29.50	36.53	8.40
	400	40.80	45.20	5.60	35.20	31.70	40.40	5.60
	600	41.20	61.60	8.00	35.60	36.60	46.13	8.00
	800	49.20	50.40	7.20	26.00	33.20	41.87	7.20
	1200	44.00	53.20	5.60	38.80	35.40	45.33	5.60
	1600	48.80	53.60	6.00	26.00	33.60	42.80	6.00
	2187	49.60	62.00	5.20	41.60	39.60	51.07	5.20
CoT-SFT	100	47.20	50.00	28.80	25.60	37.90	40.93	28.80
	200	56.00	52.40	38.00	34.00	45.10	47.47	38.00
	400	55.20	57.20	22.40	30.40	41.30	47.60	22.40
	600	58.40	55.20	24.00	35.60	43.30	49.73	24.00
	800	57.60	47.60	26.80	41.60	43.40	48.93	26.80
	1200	58.00	54.40	35.60	32.40	45.10	48.27	35.60
	1600	53.20	58.40	33.20	40.40	46.30	50.67	33.20
	2187	53.60	58.80	36.80	36.80	46.50	49.73	36.80
Reason-RFT-Zero	100	46.00	65.20	6.80	58.80	44.20	56.67	6.80
	200	48.80	66.00	9.20	57.60	45.40	57.47	9.20
	400	42.00	71.20	8.40	50.80	43.10	54.67	8.40
	600	47.20	65.20	7.60	47.60	41.90	53.33	7.60
	800	56.40	69.20	6.80	55.20	46.90	60.27	6.80
	1200	52.00	73.60	7.20	59.20	48.00	61.60	7.20
	1600	51.60	71.60	6.40	54.80	46.10	59.33	6.40
	2500	49.60	71.20	5.20	53.20	44.80	58.00	5.20
Reason-RFT	100	59.20	57.60	38.00	41.60	49.10	52.80	38.00
	200	59.60	64.40	39.20	42.00	51.30	55.33	39.20
	400	61.60	64.00	39.20	37.20	50.50	54.27	39.20
	600	66.80	67.20	32.00	46.00	53.00	60.00	32.00
	800	66.00	65.60	34.00	39.20	51.20	56.93	34.00
	1200	67.20	65.20	33.60	40.80	51.70	57.73	33.60
	1600	63.60	66.00	33.20	44.80	51.90	58.13	33.20
	2500	68.00	67.20	28.40	44.80	52.10	60.00	28.40

Table 11: Complete experimental results of Qwen2VL-2B-Instruct on the Super-Clevr-Math test set after training on Clevr-Math. “add-sub” denotes the addition-subtraction task, while “sub-multi” denotes the subtraction-multiphop task. “Direct Arithmetic”(DS-D) refers to the types of questions the model has previously seen during Clevr-Math training, while “Mixed Arithmetic”(DS-M) denotes the complicated types that the model has not encountered (*i.e.* questions with multi-step mixture of addition and subtraction).

Methods	Steps	Visual Counting				
		Clevr-Math (ID)				
		adversarial	sub-multi	addition	subtraction	AVG
Zero-Shot	-	99.60	98.40	97.60	98.80	98.60
ANS-SFT	100	69.20	54.00	81.20	69.20	68.40
	200	61.20	50.00	82.40	75.60	67.30
	400	69.20	63.60	89.20	77.60	74.90
	600	70.40	54.00	90.40	81.20	74.00
	800	80.00	74.00	91.20	89.20	83.60
	1200	86.80	79.20	94.40	91.20	87.90
	1600	90.40	84.40	95.20	92.00	90.50
	2187	96.80	89.20	96.80	97.20	95.00
	100	81.60	63.60	91.20	83.60	80.00
CoT-SFT	200	80.00	64.00	92.00	88.80	81.20
	400	72.40	66.00	88.80	79.60	76.70
	600	77.60	66.00	94.40	89.20	81.80
	800	78.40	65.20	94.00	87.20	81.20
	1200	79.60	76.80	92.40	88.00	84.20
	1600	86.40	78.00	92.80	93.20	87.60
	2187	87.20	78.80	93.60	89.60	87.30
	100	98.00	94.40	98.80	99.60	97.70
	200	99.60	93.20	99.20	100.00	98.00
Reason-RFT-Zero	400	99.60	95.20	99.60	98.80	98.30
	600	98.00	98.40	100.00	99.60	99.00
	800	99.60	98.40	99.60	98.80	99.10
	1200	100.00	98.00	99.60	99.20	99.20
	1600	99.60	97.60	100.00	99.20	99.10
	2500	99.60	98.40	100.00	99.60	99.40
	100	88.80	79.20	95.60	94.40	89.50
	200	92.00	80.00	96.40	95.20	90.90
	400	94.40	84.40	96.00	95.60	92.60
Reason-RFT	600	92.80	84.00	96.40	97.60	92.70
	800	92.80	85.20	96.80	96.40	92.80
	1200	94.80	89.60	97.20	97.60	94.80
	1600	94.80	86.40	97.60	97.20	94.00
	2500	96.80	88.40	99.20	98.00	95.60

Table 12: Complete experimental results of Qwen2VL-7B-Instruct on the Clevr-Math test set after training on Clevr-Math. “sub-multi” donates the subtraction-multihop task.

Methods	Steps	Visual Counting						
		Super-Clevr-Math (DS)						
		addition	subtraction	add-sub	sub-multi	AVG	DS-D	DS-M
Zero-Shot	-	46.80	75.20	4.80	41.60	42.10	54.53	4.80
ANS-SFT	100	57.60	41.20	5.60	46.40	37.70	48.40	5.60
	200	42.00	38.80	8.00	33.60	30.60	38.13	8.00
	400	37.20	46.40	5.20	31.60	30.10	38.40	5.20
	600	32.00	44.80	12.40	19.20	27.10	32.00	12.40
	800	38.80	38.00	6.80	37.20	30.20	38.00	6.80
	1200	42.00	42.80	12.80	32.00	32.40	38.93	12.80
	1600	36.40	48.40	11.20	17.20	28.30	34.00	11.20
	2187	39.60	58.80	8.00	29.20	33.90	42.53	8.00
CoT-SFT	100	60.00	63.60	44.00	41.60	52.30	55.07	44.00
	200	67.60	66.40	48.00	46.80	57.20	60.27	48.00
	400	55.20	60.40	19.60	42.00	44.30	52.53	19.60
	600	64.80	61.20	35.20	43.20	51.10	56.40	35.20
	800	60.00	53.60	37.60	42.40	48.40	52.00	37.60
	1200	51.20	56.00	35.20	39.60	45.50	48.93	35.20
	1600	53.20	56.40	34.40	35.20	44.80	48.27	34.40
	2187	51.60	51.60	33.60	32.80	42.40	45.33	33.60
Reason-RFT-Zero	100	58.80	82.80	24.00	62.40	57.00	68.00	24.00
	200	56.00	83.20	18.80	50.00	52.00	63.07	18.80
	400	62.40	79.60	22.80	37.60	50.60	59.87	22.80
	600	61.20	85.20	17.20	49.20	53.20	65.20	17.20
	800	52.80	86.80	20.40	52.00	53.00	63.87	20.40
	1200	53.60	83.20	19.20	46.80	50.70	61.20	19.20
	1600	61.20	84.80	18.40	43.20	51.90	63.07	18.40
	2500	59.20	86.40	21.20	45.20	53.00	63.60	21.20
Reason-RFT	100	53.60	56.80	33.20	39.60	45.80	50.00	33.20
	200	52.00	61.20	31.60	44.00	47.20	52.40	31.60
	400	56.00	59.60	30.80	45.20	47.90	53.60	30.80
	600	56.00	64.00	31.60	50.00	50.40	56.67	31.60
	800	56.00	60.00	28.00	41.60	46.40	52.53	28.00
	1200	66.00	65.60	38.00	50.40	55.00	60.67	38.00
	1600	64.40	59.60	32.40	48.80	51.30	57.60	32.40
	2500	62.80	60.80	35.60	44.80	51.00	56.13	35.60

Table 13: Complete experimental results of Qwen2VL-7B-Instruct on the Super-Clevr test set after training on Clevr-Math. “add-sub” donates the addition-subtraction task, while “sub-multi” donates the subtraction-multiphop task. “Direct Arithmetic”(DS-D) refers to the types of questions the model has previously seen during Clevr-Math training, while “Mixed Arithmetic”(DS-M) denotes the complicated types that the model has not encountered (*i.e.* questions with multi-step mixture of addition and subtraction).

Methods	Steps	Structure Perception					
		Geometry3k (DS)			GeoMath (ID)		
		CHOICE	NON-CHOICE	AVG	CHOICE	NON-CHOICE	AVG
Zero-Shot	-	40.25	1.00	20.63	35.57	20.31	25.86
ANS-SFT	100	35.25	16.25	25.75	58.72	29.89	40.37
	200	33.25	17.50	25.38	56.38	35.44	43.05
	400	30.75	17.00	23.88	64.77	35.06	45.86
	600	-	-	-	73.83	38.12	51.10
	800	32.75	16.00	24.38	72.15	36.40	49.39
	1200	-	-	-	73.83	35.44	49.39
	1600	29.00	16.00	22.50	74.83	37.36	50.98
	1686	28.75	16.25	22.50	74.83	37.93	51.34
	100	16.50	21.50	19.00	31.54	34.10	33.17
CoT-SFT	200	7.50	23.50	15.50	32.89	35.25	34.39
	400	21.50	21.25	21.38	41.61	40.04	40.61
	600	-	-	-	43.62	36.59	39.14
	800	16.50	23.50	20.00	45.97	39.27	41.70
	1200	-	-	-	53.02	40.04	44.76
	1600	24.25	24.00	24.13	53.69	37.93	43.66
	1686	26.75	23.75	25.25	51.34	38.31	43.05
	100	32.25	17.75	25.00	41.61	31.23	35.00
Reason-RFT-Zero	200	33.00	18.50	25.75	48.99	35.06	40.12
	400	41.50	23.50	32.50	52.68	34.87	41.34
	600	37.00	22.75	29.88	60.74	37.55	45.98
	800	42.25	25.00	33.63	62.42	40.42	48.42
	1200	43.00	23.75	33.38	61.07	39.66	47.44
	1600	42.75	22.25	32.50	63.09	38.31	47.32
	1610	43.25	21.75	32.50	63.09	38.89	47.68
	100	37.50	23.25	30.38	50.34	41.00	44.39
	200	33.50	29.25	31.38	56.71	40.04	46.10
Reason-RFT	400	38.25	28.75	33.50	56.38	39.27	45.49
	600	40.50	27.25	33.88	61.41	41.19	48.54
	800	41.25	29.50	35.38	58.05	41.19	47.32
	1200	40.25	31.00	35.63	61.74	42.34	49.39
	1600	38.00	29.25	33.63	62.08	43.10	50.00
	1610	36.75	29.50	33.13	60.74	42.34	49.03

Table 14: Complete experimental results of Qwen2VL-2B-Instruct on the Structure Perception task after training on GeoMath.

Methods	Steps	Structure Perception					
		Geometry3k (DS)			GeoMath (ID)		
		CHOICE	NON-CHOICE	AVG	CHOICE	NON-CHOICE	AVG
Zero-Shot	-	45.25	23.00	34.13	61.07	38.12	46.46
ANS-SFT	100	38.50	18.25	28.38	64.77	34.87	45.74
	200	32.50	22.75	27.63	69.46	35.25	47.68
	400	-	-	-	72.48	40.42	52.07
	600	32.25	18.00	25.13	73.49	39.27	51.71
	800	-	-	-	75.50	37.93	51.58
	1200	32.50	18.50	25.50	75.84	37.74	51.59
	1600	32.50	18.25	25.38	75.84	37.36	51.34
	1686	18.25	38.75	28.50	38.59	42.72	41.22
	100	6.50	32.00	19.25	38.26	43.10	41.34
CoT-SFT	200	27.00	34.50	30.75	56.71	44.64	49.03
	400	-	-	-	52.68	44.06	47.19
	600	35.50	36.25	35.88	63.09	43.49	50.61
	800	-	-	-	63.42	42.91	50.36
	1200	29.50	37.50	33.50	64.09	44.06	51.34
	1600	29.25	36.75	33.00	61.74	44.06	50.49
	1686	58.50	41.75	50.13	56.71	45.98	49.88
	100	59.00	44.25	51.63	63.42	45.21	51.83
	200	62.00	43.00	52.50	70.47	45.40	54.51
Reason-RFT-Zero	400	-	-	-	70.13	46.74	55.24
	600	64.75	45.25	55.00	70.47	49.23	56.95
	800	-	-	-	66.11	46.17	53.42
	1200	69.00	43.25	56.13	71.14	45.59	54.88
	1600	66.25	43.25	54.75	69.80	46.55	55.00
	1610	46.75	37.50	42.13	67.79	45.79	53.79
	100	53.00	37.00	45.00	72.82	46.93	56.34
	200	52.75	37.25	45.00	71.14	46.55	55.49
	400	51.50	37.00	44.25	73.49	48.28	57.44
Reason-RFT	600	56.75	37.25	47.00	77.52	46.17	57.56
	800	59.00	40.00	49.50	79.87	48.08	59.63
	1200	56.00	39.50	47.75	74.50	49.62	58.66
	1600	59.00	39.50	49.25	78.52	48.28	59.27
	1610	59.00	39.50	49.25	78.52	48.28	59.27

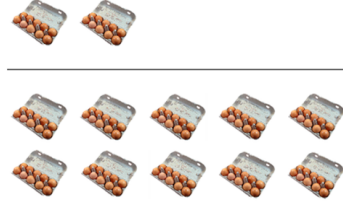
Table 15: Complete experimental results of Qwen2VL-7B-Instruct on the Structure Perception task after training on GeoMath.

Method	Steps	TRANCE (ID)								Spatial Transformation						TRANCE-R (DS-R)			
		Level-1	Level-2	Level-3	Level-4	Avg	Level-1	Level-2	Level-3	Level-4	Avg	Level-1	Level-2	Level-3	Level-4	Avg			
GPT-4o Zero-Shot	/	47.28	42.96	40.87	39.08	42.55	23.16	30.56	30.73	30.22	28.67	24.38	31.74	31.13	31.77	29.76			
	/	2.10	3.27	4.08	5.68	3.78	2.02	4.73	5.57	6.08	4.60	2.39	4.73	5.59	5.95	4.67			
ANS-SFT	100	15.90	19.12	14.67	13.12	15.70	10.60	11.33	10.01	9.07	10.25	11.08	12.17	10.17	10.07	10.87			
	200	23.97	29.56	33.98	33.95	30.37	13.25	26.76	31.26	32.58	25.96	13.53	26.54	30.53	31.20	25.45			
	400	44.95	42.58	40.75	33.65	40.48	26.03	35.98	34.26	29.38	31.41	24.06	35.62	35.46	31.73	31.72			
	800	62.10	56.55	53.01	47.55	54.80	24.70	42.27	43.05	42.65	38.17	26.09	38.98	42.95	42.55	37.64			
	1600	80.70	75.68	68.34	64.60	72.33	34.38	49.00	53.83	53.10	47.58	35.84	49.28	51.23	52.50	47.21			
	3200	82.85	80.30	78.00	71.60	78.19	36.22	52.61	55.23	54.27	49.58	38.51	52.78	54.47	53.98	49.94			
COT-SFT	final	82.70	79.93	76.70	70.22	77.39	36.00	52.82	54.59	53.55	49.24	39.63	53.75	54.33	53.60	50.33			
	100	6.99	14.90	15.99	20.36	14.56	10.32	13.74	11.82	14.69	12.64	6.97	13.38	12.84	13.41	11.65			
	200	15.45	19.12	14.53	16.46	16.39	12.90	17.51	14.22	15.82	15.11	11.23	17.71	13.87	16.32	14.78			
	400	25.98	26.74	19.94	16.02	22.17	15.73	21.19	17.73	15.96	17.65	16.13	20.55	17.91	15.97	17.64			
	800	43.85	43.19	41.77	37.84	41.66	22.88	38.29	37.54	35.29	33.50	22.74	35.81	37.60	36.23	33.10			
	1600	52.82	61.06	54.38	45.85	53.53	28.65	43.95	40.99	40.13	38.43	29.00	41.23	40.78	39.26	37.57			
Reason-RFT-Zero	3200	61.40	69.15	65.32	62.28	64.54	28.67	45.97	50.06	52.10	44.20	31.19	45.87	45.92	51.35	43.58			
	final	67.47	67.52	62.78	59.70	64.37	28.87	44.41	49.16	50.30	43.19	30.20	44.77	47.15	49.33	42.86			
Reason-RFT	100	8.44	17.96	20.69	26.22	18.33	8.53	17.42	21.16	21.05	18.04	8.08	18.12	21.09	25.70	18.25			
	200	9.59	18.76	22.97	28.73	20.01	9.49	20.08	23.19	27.00	19.94	9.72	18.97	22.82	28.50	20.00			
	400	12.35	21.47	27.01	26.25	21.77	11.10	21.47	25.73	25.30	20.90	10.54	21.19	25.44	25.60	20.69			
	800	18.47	32.08	32.77	27.85	27.79	15.40	29.12	30.93	27.38	25.71	15.52	27.75	31.50	27.88	25.66			
	1600	36.78	40.20	37.78	34.51	37.32	19.96	33.03	35.84	34.49	30.83	20.39	32.85	33.87	33.90	30.25			
	3200	43.72	46.89	44.07	40.50	43.80	18.67	34.11	37.85	39.69	32.58	18.08	34.01	37.27	40.27	32.41			
Reason-RFT-Zero	46.21	45.01	44.53	42.11	44.47	18.33	34.57	37.94	40.57	32.85	18.28	33.45	37.44	40.34	32.38				
Reason-RFT	100	53.52	55.47	58.91	53.35	55.31	31.84	47.02	50.62	50.39	44.97	31.29	46.08	48.61	49.85	43.96			
	200	54.97	59.77	63.67	59.46	59.47	35.72	49.28	54.85	54.67	48.63	36.74	52.27	53.68	54.16	49.21			
	400	63.80	66.97	68.47	64.70	65.99	39.74	55.94	61.27	57.94	53.72	41.10	56.35	59.16	57.22	53.46			
	800	64.33	68.13	66.88	63.15	65.62	47.40	61.64	63.00	58.45	57.62	46.76	60.60	61.40	59.91	57.17			
	1600	76.47	73.42	74.05	69.16	73.28	52.68	62.22	66.56	64.71	61.54	53.47	65.17	64.98	63.52	61.79			
	3200	72.88	74.85	75.77	72.45	73.99	52.58	63.60	68.51	66.01	62.68	52.67	65.60	67.60	65.66	62.88			
	final	74.10	74.52	76.68	73.12	74.61	53.49	65.72	69.64	67.34	64.05	54.95	66.25	68.32	66.80	64.08			

Table 16: Complete experimental results of Qwen2VNL-2B-Instruct on the Spatial Transformation task after training on TRANCE.

Method	Steps	Spatial Transformation										TRANCE-R (DS-R)				
		TRANCE (ID)										TRANCE-L (DS-L)				
		Level-1	Level-2	Level-3	Level-4	Avg	Level-1	Level-2	Level-3	Level-4	Avg	Level-1	Level-2	Level-3	Level-4	Avg
GPT-4o Zero-Shot	/	47.28	42.96	40.87	39.08	42.55	23.16	30.56	30.73	30.22	28.67	24.38	31.74	31.13	31.77	29.76
	/	16.25	16.42	10.96	10.48	13.53	11.71	16.80	11.50	10.85	12.72	13.30	16.08	10.55	11.18	12.78
ANS-SFT	100	40.30	37.05	30.67	28.35	34.09	32.07	31.12	26.00	26.80	29.00	26.38	29.71	27.74	26.48	27.58
	200	65.18	53.33	49.43	45.15	53.27	33.29	45.14	45.61	45.52	42.39	35.17	43.43	45.97	43.02	41.90
COT-SFT	400	65.33	59.35	57.17	50.77	58.16	32.40	44.13	47.69	46.23	42.61	32.10	44.88	47.04	45.25	42.32
	800	78.90	70.67	63.97	62.10	68.91	34.08	50.62	51.99	52.95	47.41	34.22	50.40	50.62	52.88	47.03
Reason-RFT-Zero	1600	78.50	76.12	73.80	66.25	73.67	38.85	52.97	57.93	56.05	51.45	37.77	53.57	56.45	55.92	50.93
	3200	83.80	83.23	82.83	78.17	82.01	40.10	56.02	61.02	59.90	54.26	40.78	55.06	61.67	60.98	54.62
Reason-RFT	final	83.70	84.10	82.50	78.45	82.19	39.67	55.58	61.84	60.05	54.29	42.64	54.84	61.44	60.38	54.83
	100	20.58	28.98	25.97	30.00	26.38	21.89	29.94	29.18	29.33	27.59	18.49	28.43	30.43	30.36	26.93
Reason-RFT-Zero	200	41.80	44.08	46.02	42.16	43.52	25.31	36.28	36.81	38.86	34.32	21.19	34.55	37.06	37.54	32.59
	400	45.39	51.32	58.20	52.42	51.83	32.53	44.61	47.73	46.10	42.74	31.87	38.96	44.62	45.90	40.34
Reason-RFT	800	54.87	61.97	62.20	59.93	59.74	30.19	46.01	50.01	52.88	44.77	29.91	45.02	49.60	52.83	44.34
	1600	71.27	71.14	72.82	69.93	71.29	28.82	46.43	51.01	58.94	46.30	29.08	45.25	52.24	58.31	46.22
Reason-RFT	3200	84.13	80.62	79.99	78.42	80.79	29.93	47.63	56.49	62.54	49.15	30.46	47.85	54.83	61.02	48.54
	final	86.50	79.43	80.54	78.77	81.31	28.07	47.54	54.42	61.58	47.90	29.69	45.32	54.69	61.48	47.80
Reason-RFT	100	23.59	31.62	33.22	31.27	29.93	15.88	26.86	28.13	30.19	25.27	15.21	27.29	27.54	29.88	24.98
	200	35.06	39.45	36.80	34.77	36.52	20.39	30.22	31.15	31.20	28.24	18.10	29.27	30.57	30.81	27.19
Reason-RFT	400	45.28	40.78	41.70	35.35	35.78	20.20	39.28	35.43	33.44	32.09	21.72	39.47	37.63	32.79	32.90
	800	50.18	51.55	50.43	46.06	49.56	35.44	46.15	45.65	39.55	41.70	33.90	45.89	46.48	41.57	41.96
Reason-RFT	1600	59.60	61.90	57.30	55.36	58.54	43.95	55.03	52.96	50.60	50.64	41.28	56.46	51.64	49.08	49.62
	3200	62.50	68.53	68.79	66.22	66.51	42.54	58.05	58.97	60.10	54.92	42.56	56.93	60.02	60.21	54.93
Reason-RFT	final	65.63	68.30	69.45	67.30	67.67	46.61	58.22	61.69	62.26	57.20	45.53	58.40	61.81	58.85	56.15
Reason-RFT	100	60.07	62.95	68.53	62.78	63.58	37.09	52.54	60.21	54.99	51.21	35.26	52.56	57.30	55.42	50.14
	200	67.69	66.98	69.53	66.00	67.55	36.26	53.94	60.20	60.05	52.61	34.33	54.21	58.25	60.79	51.90
Reason-RFT	400	74.72	71.31	73.62	69.14	72.20	36.11	56.00	62.25	63.01	54.34	36.95	55.72	60.82	64.88	54.59
	800	72.57	71.04	75.58	73.26	73.11	38.93	56.86	64.10	63.69	55.90	35.06	54.39	60.82	64.88	53.79
Reason-RFT	1600	79.18	76.70	76.59	73.26	76.43	37.25	53.44	66.38	66.76	55.96	35.01	55.39	66.02	66.67	55.77
	3200	79.70	79.22	80.13	76.61	78.92	37.63	55.73	65.24	68.02	56.66	37.18	56.34	63.90	68.89	56.58
Reason-RFT	final	80.48	79.15	81.97	78.26	79.97	43.68	61.04	64.66	68.05	59.36	45.45	56.34	63.33	69.33	58.61

Table 17: Complete experimental results of Qwen2VNL-7B-Instruct on the Spatial Transformation task after training on TRANCE.



COT-SFT:

<think>First, let's count the number of egg trays in the first group. There are 3 trays in the first group. Each tray holds 12 eggs, so the total number of eggs in the first group is $3 \text{ trays} * 12 \text{ eggs/tray} = 36 \text{ eggs}$. Next, let's count the number of egg trays in the second group. There are 10 trays in the second group. Each tray holds 12 eggs, so the total number of eggs in the second group is $10 \text{ trays} * 12 \text{ eggs/tray} = 120 \text{ eggs}$. Now, let's find the ratio of the total number of eggs in the second group to the first group: $120 \text{ eggs} / 36 \text{ eggs} = 10$. Therefore, the second group has 10 times more eggs than the first group.</think>

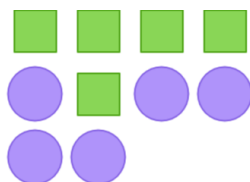
<answer>10</answer>

Question: How many times larger is the total number of eggs in the second group compared to the first group?

Reason-RFT:

<think>First, let's count the number of egg trays in the first group. There are 2 trays in the first group. Each tray contains 10 eggs, so the total number of eggs in the first group is $2 \text{ trays} * 10 \text{ eggs/tray} = 20 \text{ eggs}$. Next, let's count the number of egg trays in the second group. There are 10 trays in the second group. Each tray contains 10 eggs, so the total number of eggs in the second group is $10 \text{ trays} * 10 \text{ eggs/tray} = 100 \text{ eggs}$. Now, let's compare the total number of eggs in the second group to the first group. The second group has 100 eggs, and the first group has 20 eggs. To find how many times larger the second group is compared to the first group, we divide the total number of eggs in the second group by the total number of eggs in the first group: $100 \text{ eggs} / 20 \text{ eggs} = 5$.</think>

<answer>5</answer>



COT-SFT:

<think>First, let's count the number of green squares. There are 4 green squares in the image. Next, let's count the number of purple circles. There are 5 purple circles in the image. To find the difference, we subtract the number of green squares from the number of purple circles: $5 \text{ (purple circles)} - 4 \text{ (green squares)} = 1$.</think>

<answer>1</answer>

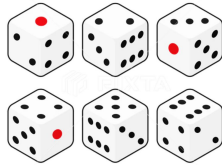
Question: How many more purple circles are there than green squares?

Reason-RFT:

<think>First, let's count the number of purple circles. I see 1, 2, 3, 4, 5 purple circles. Next, let's count the number of green squares. I see 1, 2, 3, 4, 5 green squares. Now, to find out how many more purple circles there are than green squares, we subtract the number of green squares from the number of purple circles: $5 \text{ (purple circles)} - 5 \text{ (green squares)} = 0$. Oh, I see, there are no more purple circles than green squares.</think>

<answer>0</answer>

Figure 15: Visualization examples of Reason-RFT and CoT-SFT on general visual reasoning.



Question: Based on the image, determine which number is directly opposite to number 4 on the die depicted. Use reasoning to arrive at the correct answer from the choices provided.

Choices: A. 1 B. 2 C. 3 D. 6

COT-SFT:

<think>Let me think about the properties of a standard six-sided die. On a six-sided die, each number from 1 to 6 is opposite to another number. **The sum of the numbers on opposite sides is always 7. Number 4 is opposite to number 2 because $4 + 2 = 6$, and the sum of 6 and 1 is 7. Therefore, the number directly opposite to number 4 is 2.</think>**

<answer>B</answer>

Reason-RFT:

<think>Let's analyze the image. The numbers shown are 2, 3, and 4. To find the number opposite to 4, we need to consider the properties of a standard six-sided die. **On a die, opposite numbers add up to 7. Since 4 is opposite to 3, we can conclude that the number opposite to 4 is 3.</think>**

<answer>C</answer>



Question: What is the total surface area of this rectangular prism if its dimensions are 3 units by 4 units by 5 units?

COT-SFT:

<think>To find the total surface area of a rectangular prism, we need to calculate the sum of the areas of all six faces. **The formula for the surface area is $2 * (\text{length} * \text{width} + \text{width} * \text{height} + \text{height} * \text{length})$. Let's calculate it step-by-step. 1. Calculate the area of the face with dimensions 3 units by 4 units: $3 * 4 = 12$ square units. 2. Calculate the area of the face with dimensions 4 units by 5 units: $4 * 5 = 20$ square units. 3. Calculate the area of the face with dimensions 5 units by 3 units: $5 * 3 = 15$ square units. Now, add these areas together: $12 + 20 + 15 = 47$ square units.**

Therefore, the total surface area of the rectangular prism is 47 square units.</think>

<answer>47</answer>

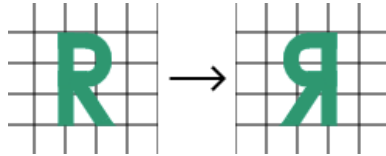
Reason-RFT:

<think>To find the total surface area of a rectangular prism, we need to calculate the sum of the areas of all six faces. **The formula for the total surface area is $2 * (\text{length} * \text{width} + \text{width} * \text{height} + \text{height} * \text{length})$. Let's calculate it step by step. First, calculate the area of the face with dimensions 3 units and 4 units: $3 * 4 = 12$ square units. Next, calculate the area of the face with dimensions 4 units and 5 units: $4 * 5 = 20$ square units. Then, calculate the area of the face with dimensions 5 units and 3 units: $5 * 3 = 15$ square units. Now, add these areas together: $12 + 20 + 15 = 47$ square units.**

Finally, multiply by 2 to account for both pairs of each face: $2 * 47 = 94$ square units.</think>

<answer>94</answer>

Figure 16: Visualization examples of Reason-RFT and CoT-SFT on general visual reasoning.



COT-SFT:

<think>Let me think about the transformation applied to the letter on the left. The letter on the left is a grid of squares, and the letter on the right is also a grid of squares. **The orientation and shape of the letter remain the same**, but the position of the letter has changed. Oh, I see, **this is a slide transformation because the letter has been moved horizontally.** </think>

<answer>A</answer>

Question: What the transformation has been applied to the letter on the left to obtain the letter on the right, and which option correctly describes this transformation?

Choices: (A) slide (B) flip (C) turn

Reason-RFT:

<think>Let's analyze the image. The letter on the left is the original image, and the letter on the right is the transformed image. **The transformation involves flipping the letter horizontally.** This means the letter has been **mirrored along a vertical axis.** Therefore, the correct option describing **this transformation is a flip.** </think>

<answer>B</answer>

Kilometers walked	
Day	Kilometers
Monday	4
Tuesday	3
Wednesday	7
Thursday	4
Friday	7
Saturday	3
Sunday	7

COT-SFT:

<think>First, let's list the kilometers Josiah walked each day: 4, 3, 7, 4, 7, 3, 7. Now, let's count how many times each number appears: **4 appears 3 times**, **3 appears 2 times**, and **7 appears 2 times**. Oh, I see, the number that appears the most frequently is the mode. **Since 4 appears 3 times, which is more than any other number, the mode is 4.** </think>

<answer>4</answer>

Question: Josiah kept track of how many kilometers he walked during the past 7 days. Can you determine which number of kilometers he walked most frequently?

Reason-RFT:

<think>First, let's list the kilometers Josiah walked each day: 4, 3, 7, 4, 7, 3, 7. Now, let's count how many times each distance appears: **- 4 km appears 2 times**. **- 3 km appears 2 times**. **- 7 km appears 3 times**. Oh, I see, **the highest frequency is 3, which corresponds to 7 km.** </think>

<answer>7</answer>

Figure 17: Visualization examples of Reason-RFT and CoT-SFT on general visual reasoning.

**COT-SFT:**

<think>Let me think about the main structural elements visible in the image. **First, I notice the two large white towers, which are the main supports for the suspension bridge.** These towers are tall and robust, providing the necessary height and strength to maintain the tension in the cables. **So, there are two main structural elements: the towers.** Oh, I see, the towers are crucial for supporting the weight of the bridge and ensuring its stability. Without them, the bridge would not be able to span the valley effectively.</think>

<answer>2</answer>

Question: How many main structural elements can be identified in the suspension bridge, and what are their roles in supporting the bridge?

Reason-RFT:

<think>Let me think about the main structural elements visible in the image. **First, I notice the two large towers supporting the bridge.** These towers are crucial for providing the necessary height and strength to maintain the bridge's structure. **Next, I see the main span of the bridge, which is the horizontal part connecting the towers.** This span is supported by the towers and is essential for carrying the weight of the bridge and any traffic it carries. **Finally, there are additional support structures visible, such as the curved steel cables,** which help distribute the weight evenly and maintain the bridge's stability. So, the main structural elements are the towers, the main span, and the curved steel cables. Counting these elements, I see two towers, one main span, and multiple curved steel cables. **Therefore, the main structural elements are three: the towers, the main span, and the curved steel cables.**</think>

<answer>3</answer>



Question: How many distinct colors of lights are used in the Christmas tree decoration?

COT-SFT:

<think>Let me think about the colors described in the image. **The Christmas tree is decorated with lights that are described as being red, blue, and white.** I need to count these distinct colors. First, I identify the color red, which is mentioned directly. Next, I see the color blue, which is also mentioned. Finally, I observe the color white, which is described as shining brightly. **So, there are three distinct colors of lights used in the decoration: red, blue, and white.**</think>

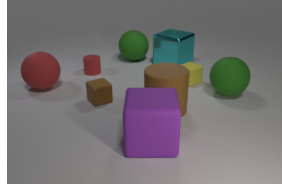
<answer>3</answer>

Reason-RFT:

<think>Let me think. The image shows a Christmas tree decorated with lights. The description mentions that the lights are of different colors. I need to identify these colors. **The description specifically mentions red and white lights.** So, there are two distinct colors of lights used in the decoration.</think>

<answer>2</answer>

Figure 18: Visualization examples of Reason-RFT and CoT-SFT on general visual reasoning.



Question: Subtract all spheres. How many objects are left?

COT-SFT:

<think>Let's start by identifying all the objects in the image. We can see various shapes: spheres, cubes, and cylinders. First, let's count the total number of objects in the image: 1. Red sphere 2. Green sphere 3. Another green sphere 4. Purple cube 5. Brown cube 6. Yellow cube 7. Brown cylinder 8. Blue transparent cube. **(Miss one object)** Now, let's identify and count the spheres: - Red sphere - Green sphere - Another green sphere. There are 3 spheres in total. Next, we subtract the number of spheres from the total number of objects: **Total objects = 8, Spheres = 3.** Objects left after subtracting spheres = **Total objects - Spheres = 8 - 3 = 5.** Oh, I see, after removing all the spheres, we are left with 5 objects.</think>

<answer>5</answer>

Reason-RFT:

<think>Let's start by identifying all the objects in the image. I see a total of 9 objects. The question asks us to subtract all the spheres.

There are 3 spheres in the image: a red sphere, a green sphere, and a green sphere. **So, we need to subtract these 3 spheres from the total of 9 objects.** $9 \text{ (total objects)} - 3 \text{ (spheres)} = 6.$ Therefore, after subtracting the spheres, there are 6 objects left.</think>

<answer>6</answer>



Question: Add 7 small cars. How many cars are left?

COT-SFT:

<think>Let's start by identifying the number of cars in the image. I see a blue SUV, a red airplane, a purple dirt bike, and a blue small car. **That makes a total of 4 cars initially.** Now, according to the question, we need to add 7 small cars to the existing ones. So, let's calculate the total number of cars after adding these 7 small cars. **Initial number of cars = 4.** Number of small cars to add = 7. Total number of cars = Initial number of cars + Number of small cars to add. **Total number of cars = 4 + 7 = 11.** Therefore, after adding 7 small cars, there are 11 cars in total.</think>

<answer>11</answer>

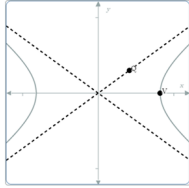
Reason-RFT:

<think>Let's start by identifying the cars in the image. I see two cars: a blue SUV and a blue minivan. The question asks to add 7 small cars to the existing cars. So, we begin with 2 cars and add 7 more.

2 (existing cars) + 7 (additional cars) = 9 cars in total. Therefore, after adding 7 small cars, there are 9 cars in total.</think>

<answer>9</answer>

Figure 19: Visualization examples of Reason-RFT and CoT-SFT on Visual Counting task.



COT-SFT:

<think>Let's think about the properties of a hyperbola. The slope of the asymptote of a hyperbola is given by the equation $m = \frac{a}{b}$, where a and b are the coefficients from the equation of the hyperbola $\frac{x^2}{a^2} - \frac{y^2}{b^2} = 1$. The distance from the center to the vertex is c , which is related to the semi-major and semi-minor axes. However, to find the equation of the hyperbola, **we need more information than just the slope of the asymptote and the distance from the center to the vertex**. We also need the values of a and b , which are not directly provided in the image. Therefore, the information given is insufficient to determine the equation of the hyperbola.</think>

<answer>B</answer>

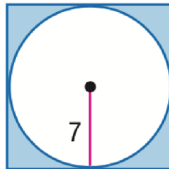
Question: Given the hyperbola shown in the image, can we determine the equation of the hyperbola by analyzing the relationship between the slope of the asymptote and the distance from the center to the vertex?

Choices: A. Yes B. No

Reason-RFT:

<think>Let's analyze the image. The hyperbola is shown with two asymptotes intersecting at the center. To find the equation of the hyperbola, we need to consider the relationship between the slope of the asymptote and the distance from the center to the vertex. The equation of a hyperbola with its center at the origin and aligned with the coordinate axes is given by $\frac{x^2}{a^2} - \frac{y^2}{b^2} = 1$, where a and b are the distances from the center to the vertices and asymptotes, respectively. The center to the vertices is given, which suggests that $a^2 + b^2$ is given. The slope of the asymptotes is given by $\pm \frac{b}{a}$. In this case, the slope is 3, which implies that $\frac{b}{a} = 3$. Therefore, the equation of the hyperbola can be determined by these relationships.</think>

<answer>A</answer>



COT-SFT:

<think>To find the circumference of the circle, I need to know the diameter of the circle. The diameter is the longest straight line that can be drawn across a circle, passing through the center. Once I have the diameter, I can use the formula for the circumference of a circle, which is $C = \pi d$, where d is the diameter. Oh, I see, the diameter of the circle is given as 7. So, I can calculate the circumference as $C = \pi * 7$. Using the value of π as approximately 3.14159, I can calculate the circumference as $7 * 3.14159 = 21.99633$. Rounding this to one decimal place, the circumference is approximately 22.</think>

<answer>22</answer>

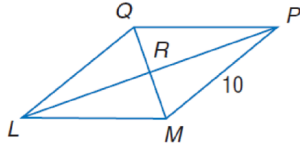
Question: What is the circumference of the circle?

Reason-RFT:

<think>First, let's determine the radius of the circle. The problem states that the radius is 7. The formula for the circumference of a circle is $C = 2 \pi r$, where r is the radius. Substituting the given radius, $r = 7$, into the formula, we have $C = 2 \pi (7)$. Calculating this gives $C = 14 \pi$. Therefore, the circumference of the circle is 14π .</think>

<answer>14 \pi</answer>

Figure 20: Visualization examples of Reason-RFT and CoT-SFT on Structure Perception task.



COT-SFT:

<think>Let's think about this step-by-step. The rhombus LMPQ is a type of quadrilateral where all sides are equal in length. We are given that side LM is 8 units long. Since all sides of a rhombus are equal, the length of side QP must also be equal to the length of side LM. Therefore, QP = LM = 8 units.</think>

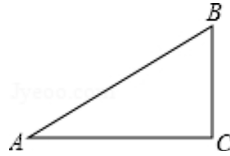
<answer>8</answer>

Question: What is the length of side QP in the rhombus?

Reason-RFT:

<think>Let's analyze the rhombus LMPQ. We know that all sides of a rhombus are equal in length. The side QP is one of these equal sides. Since the problem states that the side MP is 10, we can confirm that this is indeed the length of side QP in the rhombus LMPQ. </think>

<answer>10</answer>



COT-SFT:

<think>Let's think through this step-by-step. We know that angle A is 37 degrees, and we have the tangent function, which is the ratio of the opposite side (AB) to the adjacent side (AC). Given that $\tan(37^\circ) = 0.75$, we can write the equation as $AB = AC / \tan(37^\circ)$. Substituting the given value, $AB = 4 / 0.75$. Calculating this gives $AB = 5.33$. Now, we need to find the hypotenuse BC using the Pythagorean theorem, which states that in a right triangle, the square of the hypotenuse is equal to the sum of the squares of the other two sides. So, $BC = \sqrt{AB^2 + AC^2}$. Substituting the known values, $BC = \sqrt{5.33^2 + 4^2}$. Calculating this gives $BC = 7.34$. Therefore, the approximate length of BC is 7.34, which is not an exact match with the options. However, the closest approximation from the choices given is 3.0, which is not correct based on our calculations. Let's re-evaluate the choices and the reasoning provided.</think>

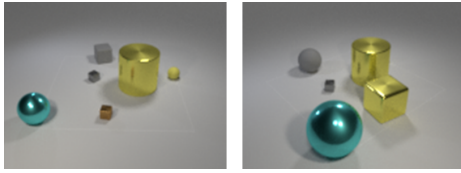
<answer>Based on the reasoning and calculations, the closest approximation from the choices given is 3.0, which is not correct based on our calculations</answer>

Reason-RFT:

<think>Let's start by finding the length of BC using the tangent of angle A. We know that $\tan(\text{angle A}) = \text{opposite} / \text{adjacent} = BC/AC$. Given that angle A is 37 degrees, we can write: $\tan(37^\circ) = BC/4$. We also know that $\tan(37^\circ)$ is approximately 0.75. So, $BC = 4 * 0.75 = 3$. Therefore, the length of BC is approximately 3.0.</think>

<answer>B</answer>

Figure 21: Visualization examples of Reason-RFT and CoT-SFT on Structure Perception task.



Initial central-view image

Final left-view image

Question: The first image shows the central view of initial state, the second image shows the left view of final state, and the attributes of the initial objects are listed below:
 (0, cube, medium, gray, rubber) (1, sphere, medium, cyan, metal)
 (2, cube, small, gray, metal) (3, cube, small, brown, metal)
 (4, cylinder, large, yellow, metal) (5, sphere, small, yellow, rubber)
 What is the transformation process that can achieve the change from initial state to final state?

COT-SFT:

<think>Let's analyze the initial and final states of the objects in the images. We have the attributes of the initial objects, and we need to determine the transformations that lead to the final state.

- **Object 0**: Initially, it's a medium gray rubber cube. In the final state, it appears to be a sphere. So, we need to change shape.
 - Transformation: `change_shape(0, sphere)`
- **Object 1**: Initially, it's a medium cyan metal sphere. In the final state, it seems to have moved to the right and increased in size.
 - Transformation: `change_position(1, right)`, `change_size(1, large)`
- **Object 2**: Initially, it's a small gray metal cube. In the final state, it appears unchanged.
- **Object 3**: Initially, it's a small brown metal cube. In the final state, it appears unchanged.
- **Object 4**: Initially, it's a large yellow metal cylinder. In the final state, it appears unchanged.
- **Object 5**: Initially, it's a small yellow rubber sphere. In the final state, it appears unchanged.

Now, let's compile the transformations needed to achieve the final state from the initial state:

- `change_shape(0, sphere)`
- `change_position(1, right)`
- `change_size(1, large)`

These transformations match the original answer provided.</think>

<answer>change_shape(0, sphere), change_position(1, right), change_size(1, large)</answer>

Reason-RFT:

<think>Let's analyze the initial and final states to determine the transformations needed.

- **Object 0**: Initially a medium gray rubber cube. In the final state, it appears to be a medium gray rubber sphere.
 - Transformation: `change_shape(0, sphere)`
- **Object 1**: Initially a medium cyan metal sphere. In the final state, it appears to be a large cyan metal sphere.
 - Transformation: `change_size(1, large)`
- **Object 2**: Initially a small gray metal cube. In the final state, it appears to be a small gray metal cube.
 - Transformation: None needed as it remains unchanged.
- **Object 3**: Initially a small brown metal cube. In the final state, it appears to be a large yellow metal cube.
 - Transformation: `change_color(3, yellow)` and `change_size(3, large)`
- **Object 4**: Initially a large yellow metal cylinder. In the final state, it appears to be a large yellow metal cylinder.
 - Transformation: None needed as it remains unchanged.
- **Object 5**: Initially a small yellow rubber sphere. In the final state, it appears to be a small yellow rubber sphere.
 - Transformation: None needed as it remains unchanged.

By analyzing the changes, we can determine the sequence of transformations needed to achieve the final state from the initial state. Therefore, the transformations are:

- `change_color(3, yellow)`
- `change_size(1, large)`
- `change_size(3, large)`
- `change_shape(0, sphere)`

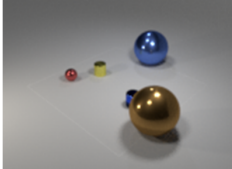
These transformations match the original answer provided. </think>

<answer>change_color(3, yellow), change_size(1, large), change_size(3, large), change_shape(0, sphere)</answer>

Figure 22: Visualization examples of Reason-RFT and CoT-SFT on Spatial Transformation task.



Initial central-view image



Final right-view image

Question: The first image shows the central view of initial state, the second image shows the right view of final state, and the attributes of the initial objects are listed below:

(0, sphere, small, red, metal)	(1, sphere, large, brown, metal)
(2, cube, large, blue, metal)	(3, sphere, small, brown, metal)
(4, cylinder, small, blue, glass)	

What is the transformation process that can achieve the change from initial state to final state?

COT-SFT:

<think>Let's analyze the initial and final states of the objects in the images. We have the initial attributes of the objects, and we need to determine the transformations that occurred.

1. **Object 0**: Initially a small red metal sphere. In the final image, it appears to have moved to the front left. So, we apply `change_position(0, front_left)`.
2. **Object 1**: Initially a large brown metal sphere. In the final image, it seems to have moved behind the other objects. So, we apply `change_position(1, behind)`.
3. **Object 2**: Initially a large blue metal cube. In the final image, it appears to have changed shape to a sphere. So, we apply `change_shape(2, sphere)`.
4. **Object 3**: Initially a small brown metal sphere. In the final image, it appears to have changed color to yellow. So, we apply `change_color(3, yellow)`.
5. **Object 4**: Initially a small blue glass cylinder. There doesn't seem to be any change in its attributes or position in final image.

Now, let's compile the transformations in the order they were identified:

- `change_color(3, yellow)`
- `change_position(0, front_left)`
- `change_shape(2, sphere)`
- `change_position(1, behind)`

These transformations match the original answer provided.</think>

<answer>change_color(3, yellow), change_position(0, front_left), change_shape(2, sphere), change_position(1, behind)</answer>

Reason-RFT:

<think>Let's analyze the initial and final states to determine the transformations needed.

1. **Object 3 (sphere, small, brown, metal):**
 - In the initial state, it is a small brown metal sphere.
 - In the final state, it appears to be a small yellow cylinder.
 - Therefore, the transformations needed are: - Change its color from brown to yellow: `change_color(3, yellow)` - Change its shape from a sphere to a cylinder: `change_shape(3, cylinder)`
2. **Object 1 (sphere, large, brown, metal):**
 - In the initial state, it is a large brown metal sphere.
 - In the final state, it has moved to the right.
 - Therefore, the transformation needed is: - Change its position to the right: `change_position(1, right)`
3. **Object 2 (cube, large, blue, metal):**
 - In the initial state, it is a large blue metal cube.
 - In the final state, it appears to be a large blue metal sphere.
 - Therefore, the transformation needed is: - Change its shape from a cube to a sphere: `change_shape(2, sphere)`

By applying these transformations, we can achieve the change from the initial state to the final state. The transformations are:

- `change_color(3, yellow)`
- `change_shape(3, cylinder)`
- `change_position(1, right)`
- `change_shape(2, sphere)`

These transformations match the original answer provided.</think>

<answer>change_color(3, yellow), change_shape(3, cylinder), change_position(1, right), change_shape(2, sphere)</answer>

Figure 23: Visualization examples of Reason-RFT and CoT-SFT on Spatial Transformation task.